

Soaking Up the Sun: Battery Investment, Renewable Energy, and Market Equilibrium

R. Andrew Butters*
Jackson Dorsey†
Gautam Gowrisankaran‡

December 14, 2021

Abstract

Renewable energy and battery storage are seen as complementary technologies that can together facilitate reductions in carbon emissions. We develop and estimate a dynamic competitive equilibrium model of storage investment and operations to evaluate the adoption trajectory of utility-scale storage under different counterfactual policy environments. Using data from California, we find that the first storage unit breaks even in 2027 when renewable energy share will reach 52%. Despite this, battery adoption is virtually non-existent until 2040 without a storage mandate or subsidy. Our model indicates this is because equilibrium effects reduce the marginal value of subsequent storage investments; expected future capital cost reductions incentivize delayed investment; and depreciation from cycling lowers the value of investment. We show that California's 2024 storage mandate decreases future electricity generation costs by \$511 million but also increases expected capital costs by \$944 million by shifting adoption earlier, before projected capital cost declines are realized.

JEL Codes: L94, Q40, Q48, Q55

Keywords: energy storage, solar PV, renewable energy, dynamic programming, electricity markets

*Department of Business Economics and Public Policy, Kelley School of Business, Indiana University (e-mail: rabutter@indiana.edu).

†Department of Business Economics and Public Policy, Kelley School of Business, Indiana University (e-mail: jfdorsey@iu.edu).

‡Department of Economics, Columbia University, NBER, and CEPR (e-mail: gautamg2@gmail.com).

We thank Jim Bushnell, Ken Gillingham, Ashley Langer, Derek Lemoine, James Mackinnon, Erin Mansur, Mar Reguant, Stan Reynolds, Mo Xiao, and numerous conference and seminar participants for helpful comments, discussions, and suggestions.

1 Introduction

Growth in renewable electricity generation has been dramatic over the past 10 years, in the U.S. and worldwide. By displacing generation from fossil fuels, renewables reduce greenhouse gas emissions. However, almost all recent growth in renewables comes from *intermittent* sources such as solar photovoltaics (PV): a solar farm cannot generate electricity after the sun sets, or when a cloud passes overhead. Absent the ability to store electricity, integrating these intermittent sources into the electricity grid requires the capability both to produce electricity at times with low expected renewable production and to adjust production suddenly when renewable production is unavailable. Intermittency reduces the benefits of renewables through the costs of building, maintaining, and operating additional fossil fuel generators (Bushnell and Novan, 2018; Gowrisankaran et al., 2016; Joskow, 2011). Thus, battery storage is a potentially important complement to intermittent renewable energy: it can lower the social costs of integrating renewables by storing energy when renewable production peaks and releasing it when it plummets.

In tandem with recent growth in renewable energy investment, the capital costs of lithium-ion battery cells fell by 85% from 2010 to 2018 with projections of 50% further cost drops over the next decade (Cole and Frazier, 2019; Goldie-Scot, 2019).¹ Despite these dramatic cost decreases, capital costs are still a central impediment to utility-scale battery storage. Moreover, even after these costs reach a break-even point, companies may defer battery investments to wait for future capital cost declines. Finally, in the long run, the equilibrium value of large-scale storage investment is limited because each additional storage unit acts as an arbitrageur, smoothing price differentials across time and lowering the value of existing units.

This paper has four main goals related to understanding the economics of battery storage. First, we evaluate the effects of utility-scale batteries in the electricity market, focusing on how their presence and operation would impact equilibrium prices, electricity generation costs, and profits for different market participants. Second, we develop a battery adoption model to understand the likely path of storage capacity that will enter over time. Third, we evaluate factors that might lead to delays in entry,

¹Other storage technologies are also expected to have up to 90% lower capital costs within the next decade (U.S. Department of Energy, 2021).

including equilibrium price effects and the expectation of future cost declines. Fourth, we evaluate the extent to which battery mandates or subsidies are necessary to achieve adoption, as well as the cost implications of these policies.

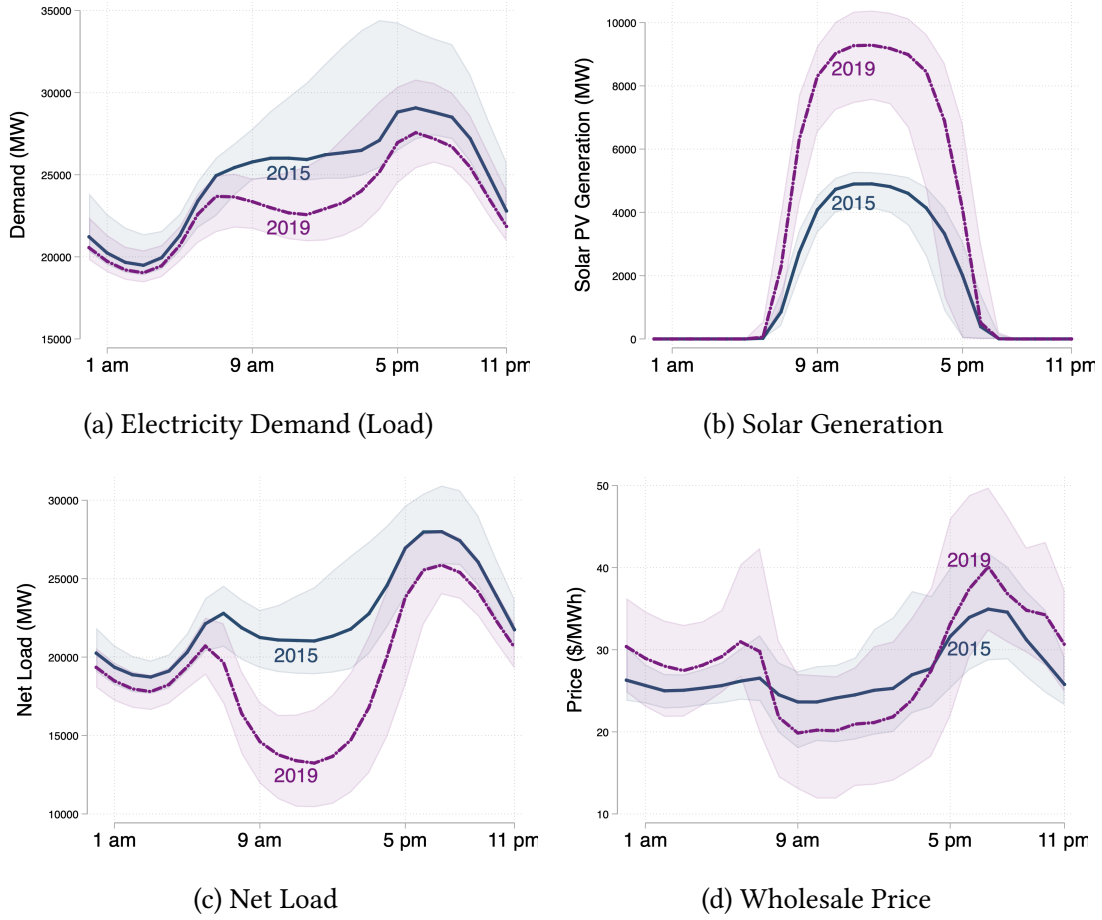
Understanding the value of policies that encourage battery storage as a complement to renewable energy is particularly important because many states have paired renewable energy mandates with battery mandates. For example, in conjunction with its aggressive renewable energy standards, California passed a requirement for utilities to procure 1,300 MW of storage power capacity by 2024.² The state justified the storage mandate on the basis that storage resources can help optimally integrate renewable energy resources and improve grid reliability. Additionally, implementing a concurrent battery mandate and renewable portfolio standard could be a cost effective way to achieve renewable energy goals if there is the potential for coordination failures at the investment stage due to these complementarities (Zhou and Li, 2018). Other states—notably Arizona, Massachusetts, New Jersey, New York, Nevada, Oregon, and Virginia—have also implemented battery procurement targets or requirements as complements to their renewable energy standards. Despite the increasing prevalence of storage mandates, little is known about the impact of these policies.

To fix ideas, we illustrate the complementarity between renewable energy and storage with California data. Figure 1a displays median electricity demand and Figure 1b displays median solar generation, over the hours of the day and separately for 2015 and 2019. Solar generation in California increased dramatically over this period, but this generation typically occurs in the middle of the day and not in the evening, when demand is highest. Figure 1c displays median *net load*, which is the difference between total demand and renewable generation, and hence the electricity that is supplied by *dispatchable generators*.³ Net load in 2019 plummets in the middle of the day but rises again in the early evening to a similar level as in 2015, resulting in a curve with two humps. This change in the shape of the net load curve has at least two implications for costs. First, it implies that solar PVs are not producing in the evening when net load, and hence marginal costs, are highest. Second, it increases the ramping costs that generators bear every time they turn on or off (Cullen, 2010; Jha and Leslie, 2020;

²This size is similar to a large natural gas power station, and could serve about 6% of typical CAISO load. With 4-hour duration batteries, it corresponds to 5,200 MWh of stored energy capacity.

³Unlike intermittent generators like wind and solar PV power plants, dispatchable generators, which include natural gas and hydroelectric plants, can be started on demand.

Figure 1: Electricity Demand, Solar Generation, and Prices by Year in California



Notes: Each panel shows the hourly median, 25th percentile, and 75th percentile of electricity demand (load), solar generation, net load, and real-time wholesale market price, respectively. Figures calculated by authors from California Independent System Operator data. All prices are for the California South Hub Trading Zone (SP15).

Mansur, 2008; Reguant, 2014). Finally, Figure 1d displays median wholesale electricity prices. Despite the similarity in evening load between 2015 and 2019, median wholesale prices are substantially higher in 2019, suggesting the importance of increased ramping costs and the potential of storage to mitigate these costs.

To incorporate key features of the electricity market, we develop a new theoretical and estimation framework with three main innovations. First, we specify and analyze a dynamic competitive *equilibrium* battery operations model that allows us to evaluate how much large-scale battery operations would affect the wholesale electricity price, and through that, limit the marginal value of additional battery capacity. Second, to solve this equilibrium operations model across different counterfactual battery

capacity levels, we develop a high-frequency time-series model of net load and the electricity generation supply curve. Our operations model and supply curve incorporate ramping costs, where past generation by dispatchable generators reduces current marginal costs. Finally, we link our operations model with a battery adoption model. In particular, our operations model microfoundations revenues for our adoption model. The adoption model in turn allows us to understand how renewable energy standards and battery mandates affect battery adoption and social surplus.

Our framework has two dynamic components: an operations model and a capacity adoption model. The operations model solves for a dynamic competitive equilibrium in charge/discharge decisions, given a fixed battery capacity level. Each five-minute interval, a fleet of battery operators buys and sells energy in the wholesale energy market. The model incorporates a number of features that we believe are important in this context: predictable within-day fluctuations in net load; a non-linear marginal cost (or supply) curve of electricity that evolves over time and includes ramping costs; serial correlation of the shocks to net load and marginal cost curve of electricity; a restriction that charge/discharge policies be based on data that would have been available in real-time to a market participant; a loss in energy from charging and discharging the battery; and the depreciation of batteries from operation, particularly with deep cycles. We estimate the electricity demand and marginal cost curves using data from the California Independent System Operator (CAISO)—which covers 80% of California’s electricity demand—from 2015-19. We estimate current and future battery capital costs from data compiled by the National Renewable Energy Laboratory (NREL).

Our capacity adoption model solves for a dynamic competitive equilibrium of investment decisions of potential battery operators. Each year, potential battery operators make an optimal stopping decision, choosing whether to install capacity or wait, given battery installation costs, current and future renewable energy standards, and the mass of existing battery capacity. The operating revenues in our capacity adoption model derive from the solution to the operations model. We solve the operations model for different in-sample levels of renewable penetration and across counterfactual battery penetration levels. We then estimate a regression that links the two models by estimating the social surplus of battery storage across these two variables.

Our results depend crucially on four main identifying assumptions. First, we as-

sume that our market price and quantity data allow us to recover the supply curve of electricity for each five-minute interval in our sample. Second, we assume that the net load process and electricity generation supply curves that we identify from the data are structural and hence will continue to hold in the presence of utility-scale batteries. This assumption implicitly rules out the possibility that fossil fuel generators will retire due to large-scale battery storage. We leverage this assumption to evaluate the marginal value of battery operations at counterfactual aggregate battery capacity levels. We allow for ramping costs, serial correlation of the residuals, and daily innovations to the supply curve. This rich dependence on observables adds to the plausibility of this assumption. Third, we identify the impact of counterfactual renewable adoption with the assumption that the relation between battery storage and renewable generation that holds in our data will continue to hold in the future when there is higher renewable penetration than exists in the data. Finally, in order to be able to solve for a dynamic competitive equilibrium, we assume that the electricity generation supply curves that we estimate represent the marginal costs of production.⁴

Relation to literature. Our study builds on three main literatures. First, it relates to an engineering and economics literature that investigates the value of storage in wholesale electricity markets. Early engineering papers in this literature modeled the storage decision using a finite-horizon framework and assumed that the storage device operator had perfect foresight about future prices or relied on historical prices when making discharge and charge decisions (e.g. [Sioshansi et al., 2009](#)). More recent engineering studies relax the perfect foresight assumption and model storage decisions given uncertainty about future prices (e.g. [Mokrian and Stephen, 2006](#)). Our operations model extends this framework by considering the equilibrium effects of large-scale storage in competitive storage markets. It also relates to two recent economics working papers. [Kirkpatrick \(2018\)](#) estimates the effect of recent utility-scale battery installations on electricity market prices and transmission line congestion in California. [Karaduman \(2021\)](#) also considers the economics of grid-scale energy stor-

⁴We leverage this assumption primarily to compute counterfactual market outcomes—specifically, generation from dispatchable generators and wholesale electricity prices—in the setting of a large battery fleet. One can also interpret our approach as recovering the more general generator supply relation in the presence of market power. Under this interpretation, our framework is still appropriate for analyzing the market impacts of a small battery fleet, and projecting when batteries would break even.

age, employing different modeling approaches and data from ours.⁵

Second, we contribute to an economics literature that explores market impacts of new energy technologies. [Wolak \(2018\)](#) and [Woo et al. \(2016\)](#) measure the environmental and market effects of renewable energy generation. [Feger et al. \(2017\)](#), [Langer and Lemoine \(2018\)](#), and [De Groote and Verboven \(2019\)](#) evaluate the impact of solar subsidies on adoption. We add to this literature with a dynamic model of investment in battery capacity, that is micro-founded with our operations model.

Third, our work also relates to the literature on electricity forecasting ([Kanamura and Ōhashi, 2007](#); [Knittel and Roberts, 2005](#); [Weron, 2014](#)) and commodity pricing ([Deaton and Laroque, 1992](#); [Pirrong, 2012](#)). Based on this literature, we develop and estimate a model of electricity load and marginal costs that allows for seasonal patterns, dynamics from ramping costs, and high-frequency cost volatility arising from unanticipated shocks to available generation.

Summary of Results. Starting with our operations model, we find that a very small battery fleet would break even—earn enough revenues in the energy market to cover costs—if capital costs were to fall by 41% from 2019 levels and renewable energy share were to increase from 40% (the share in 2019) to 52%, which are both expected to occur in 2027. A somewhat larger battery fleet with 1,000 MWh of energy capacity would reduce CAISO wholesale prices during evening hours by 6% and overall prices by 3% over our sample period. Consequently, these battery operations would improve gross social surplus by \$13 million annually through reductions in the total cost of electricity generation.⁶ Disaggregating these impacts, battery operations would reduce prices paid by utilities to serve load by \$256 million annually, provide \$14 million in annual profits for battery owners, but reduce generator profits by \$257 million. The marginal value of storage capacity increases by more than 10% when the renewable generation share increases from 40% to 50%. However, this marginal value declines sharply with aggregate battery capacity: while the first unit of storage capacity would provide over \$200/kWh in social surplus, the marginal value falls to \$125/kWh when there is 5,000 MWh of storage capacity already operating in the market. This finding highlights the importance of modeling equilibrium effects here.

⁵[Andrés-Cerezo and Fabra \(2020\)](#) investigate the influence of market structure on battery investment levels, and subsequent effects on social welfare.

⁶Gross social surplus does not account for the fixed capital costs of battery capacity.

Turning to our adoption model, we find that an ambitious renewable energy standard is not sufficient to encourage large-scale battery adoption on its own. Despite finding that a small battery adopter could break-even as soon as 2027, in the absence of California’s 2024 mandate, the battery market would not have reached the mandated level of capacity until 2044, in expectation. Three key mechanisms limit aggregate battery adoption in the absence of a mandate: (1) the equilibrium effects of battery operations greatly reduce the value of subsequent investment, (2) rapidly declining capital costs create option value that incentivizes delayed investment, and (3) battery capacity depreciation caused by charging and discharging substantially reduces the lifetime value of battery investments. All together, this set of results shows that absent a battery mandate, policymakers should expect relatively modest installed battery capacity, but also that this capacity would substantially mitigate the pattern of sharp peaks and troughs in wholesale electricity prices created by large-scale renewable generation, and thus lead to a reduction in the overall cost to serve load.

Finally, we assess the costs of meeting California’s battery mandate policy. The mandate causes earlier battery adoption, which provides electricity generation cost savings, but it increases expected capital costs by shifting battery adoption forward. We find that the 1,300 MW (5,200 MWh) mandate decreases electricity generation costs by \$511 million, but increases expected battery capital costs by \$944 million, implying a total cost of \$433 million, or \$11.50 per California resident. This figure does not include other benefits of storage—including grid reliability—that were part of the justification for the mandate.⁷

The remainder of our paper is structured as follows. Section 2 discusses our data and institutional features. Section 3 exposit our model. Section 4 explains our estimation. Section 5 presents our results and counterfactuals, and Section 6 concludes.

⁷For instance, if the presence of storage averted a single system-wide power outage for 2.2 hours in present value terms, this would add \$433 million in benefits.

2 Data and Institutional Setting

2.1 Storage Resources in the Electricity Market

Recognizing the complementarity with renewable energy, regulators nationally and in California have enacted new policies to increase electricity storage investment. In early 2018, the Federal Energy Regulatory Commission (FERC) issued Order 841, which requires independent system operators (ISO) to remove any existing barriers that would inhibit participation of storage resources in wholesale markets.

In 2010, the California legislature authorized the California Public Utility Commission (CPUC) to evaluate and determine energy storage targets for the state. Accordingly, the CPUC required the state's investor-owned utilities to procure 1.3 GW of storage power capacity by 2020,⁸ with installations required to be operational no later than the end of 2024. Since this time, California's utilities have been adding storage capacity and, by 2019, utilities had at least 126 MW of operational battery power capacity.⁹

Though energy storage technologies such as pumped hydroelectric storage have been established for decades, the majority of recent utility storage installations use battery technologies. More specifically, lithium-ion based batteries now dominate the U.S. market—accounting for over 90% of battery storage capacity (EIA, 2020). Nearly all lithium-ion battery grid resources were installed after 2014. We focus our analysis on lithium-ion batteries.

Although the stock of utility-scale batteries is growing at a rapid rate, the overall battery fleet remains small. As of 2018, there was only 900 MW of aggregate battery power capacity in the U.S., similar to that of two to three combined-cycle natural gas generators (EIA, 2020).

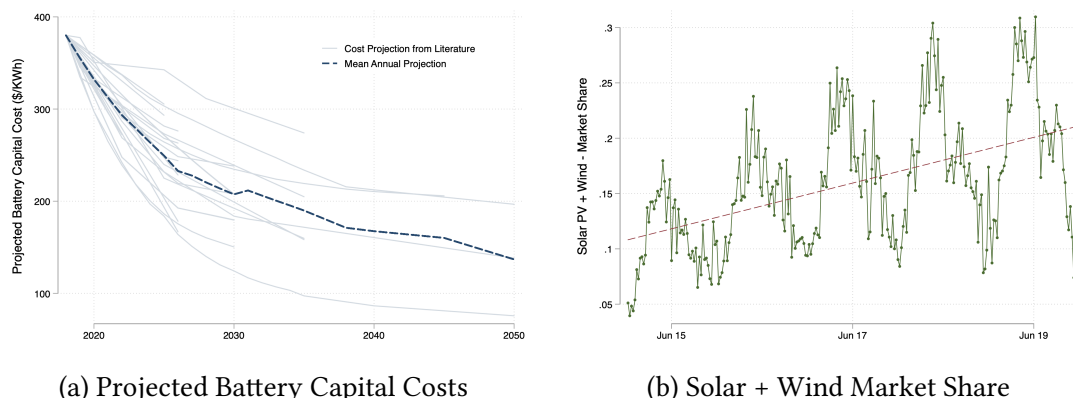
2.2 Capital Costs of Battery Storage

Our adoption model relies on data on the capital costs of energy storage. Given the large expected declines in utility-scale battery capital costs, we use forward-looking

⁸Power capacity is the amount of power that the battery can supply to the grid at any point in time while energy capacity is the maximum amount of energy that the battery can store.

⁹Authors' calculations based on maximum aggregate output reported by the California Independent System Operators between May 2018 and December 2019.

Figure 2: Battery Capital Cost Projections and Renewable Energy Trends



Notes: The authors constructed Figure 2a using data from Cole and Frazier (2019). Each transparent line represents a future cost projection from a single publication. The dashed line plots the mean cost projection. The figure reflects all cost projections related to grid battery applications (not electric cars). The authors constructed Figure 2b from CAISO data. It shows the share of electricity generation coming from solar and wind generators for each week between 2015 to 2019.

projections from the the National Renewable Energy Laboratory (Cole and Frazier, 2019) to model the evolution of future lithium-ion battery costs. These data compile utility-scale lithium-ion battery cost projections from over 25 publications published between 2016 and 2018.

Batteries vary in their round-trip efficiency and duration. A battery's round-trip efficiency measures the percentage of stored energy that is available for later usage. A battery's duration indicates the amount of time the battery is able to discharge at its rated power capacity. For example, a 2-hour duration battery could discharge at full power capacity for 2 hours. Our study follows Cole and Frazier (2019) and focuses on the most common type of battery system currently being added in U.S. markets: batteries with 4-hour duration and 85% round-trip efficiency.

Figure 2a demonstrates variation in cost projections for battery storage over time in \$/kWh. Each point in the figure represents a normalized cost projection from a single publication for one year, and the dashed line plots the mean projection by year.

2.3 The California Wholesale Electricity Market

Our operations model relies on data from the California Independent System Operator (CAISO).¹⁰ California restructured its electricity sector in 1998, and consequently designated CAISO the state’s new independent system operator. CAISO dispatches over 200 million megawatt-hours of electricity to 30 million consumers each year, accounting for about 80% of electricity demand in California. CAISO runs two distinct wholesale energy markets: a day-ahead market (DAM) and a real-time market (RTM).

In the day before power is delivered, CAISO conducts 24 DAM energy auctions, one for each hour of the day, making available projections of net load and market-clearing prices prior to the auction. Market participants then submit bids to either buy or sell energy and CAISO computes market-clearing quantities and prices that meet projected load at lowest cost.¹¹ On the day of energy delivery, CAISO uses an RTM auction 75 minutes before each delivery hour to adjust generator production in response to unplanned outages or deviations. During the delivery hour, the system operator dispatches the lowest-cost generators every five minutes. The system operator uses reserve operations to meet any unanticipated imbalance within the five minute interval.

As we discuss in Section 4, our estimation uses data from both the DAM and the RTM. We focus on wholesale electricity prices from CAISO’s South-Zone hub (SP-15), because this zone covers the largest share of the California population and currently hosts the most battery storage capacity. Additionally, we augment the electricity price data with other market data: total load from the CAISO territory, generation by resource type, natural gas prices, and hydroelectric availability.

Following FERC Order 841, CAISO has made efforts to integrate new storage technologies into its wholesale markets. CAISO allows batteries to submit either demand bids or supply bids in both day-ahead and real-time energy auctions. A battery can submit a set of prices and associated quantities at which it is willing to discharge energy, with negative quantities when it would like to charge.

Batteries also have the option to supply reserve capacity in the ancillary services market. A limitation of our approach is that we model batteries’ operations in the

¹⁰We obtained data used from the CAISO Open Access Same-time Information System (OASIS) portal. OASIS provides real-time data related to the ISO transmission system and its markets

¹¹CAISO also uses the day-ahead market to secure energy reserves.

energy market but not in the ancillary services market. Although many of the earliest battery operators provided ancillary services, it is unlikely that ancillary services will be the primary battery storage application in the long-run. Industry experts have made this point, noting that ISOs typically require only limited ancillary services capacity, on the order of 100-400 MW (Sackler, 2019).¹² For this reason, we focus our analysis on battery operations in the energy market.

Notably, California's grid is currently undertaking a dramatic transition away from fossil fuel generation and towards renewable resources that will impact storage investment and operations. As of 2015, California already hosted the largest capacity of solar PV panels in the United States. Figure 2b shows that during the sample period of our study—January 2015 to December 2019—utility-scale solar and wind resources' market share doubled from 10% to 20%, and exceeded 30% during some weeks. Going forward, state lawmakers have voted to boost renewable energy further under Senate Bill 100, signed in September 2018, which establishes the state's updated renewable portfolio standard (RPS). Figure A.2 in Online Appendix A provides details on California's RPS schedule. The law specifies the share of generation that must come from renewable sources: 44% by 2024, 52% by 2027, 60% by 2030, and 100% by 2045. The figure also projects the share of energy that will come from solar and wind together for each future year that we model, as required by our analysis. We form this projection by linearly interpolating the RPS to intermediate years, assuming that all new renewable energy will be from solar and wind, in equal proportions to the present.

Figure A.3 in Online Appendix A provides more details on market trends in CAISO over our sample period. From Figure A.3a, average demand (load) for electricity has remained relatively stable, falling by 7.5%. Figures A.3b, A.3c, and A.3d show the solar, wind, and combined solar plus wind market shares over our sample period, respectively. Average wind power production increased slightly from 5% to 7% of generation, and solar PV's generation share rose from 6% to 14%. Figure A.3e shows that prices for natural gas, the predominant fossil fuel generation source in CAISO, hovered around \$3/MMBtu for much of the sample period. Figure A.3f shows that mean prices in the real-time market have also trended upwards by nearly 20%. Finally, Figure A.4 in Online Appendix A replicates Figure 1d but with data at the five-minute,

¹²Figure A.1 in Online Appendix A shows that CAISO procured an average of less than 800 MW of hourly regulation reserves in all but five months of our five-year sample.

rather than hourly, level. It shows that real-time prices have become more volatile within each hour of the day as intermittent renewable generation has expanded and more high-frequency adjustments are required in the real-time market.

3 Model

Our dynamic equilibrium framework of battery storage includes two components. First, the *capacity adoption model* solves agents' decisions of whether to make a capital investment in storage capacity in a given year. Second, the *operations model* micro-founds the capacity adoption model by solving agents' short-run dynamic decisions regarding when to charge and discharge energy. This section describes both components, in turn.

3.1 Capacity Adoption Model

Our capacity adoption model considers an infinite mass of ex-ante identical potential battery operators, or agents for short. Each agent i has the ability to install a unit capacity of storage technology, $k = 1$, at one point in time. The unit capacity is sufficiently small that each agent takes electricity market prices as given.

Agents face an infinite horizon dynamic problem and have an annual discount factor of β . Each agent has room for one storage system and cannot replace the system once installed. Hence, agents solve an optimal stopping problem of when to invest. Adopters bear a fixed cost of obtaining storage capacity but can then use the storage capacity to earn future flow profits, by acting as arbitrageurs in the energy market.

Agent Decision Problem

At each year y , agents that have not previously adopted make a binary decision of whether or not to invest in storage capacity. Agents that adopt must pay a fixed cost, c_y , that is the cost net of any subsidy available at year y . At year y , agents observe c_y but do not know future adoption costs. We assume that these costs evolve stochastically, declining over time in expectation due to technological advances. Agents have rational expectations over future adoption costs and hence form accurate distributions over future trajectories. A benefit of waiting to invest is that capital costs are likely

to be lower in the future. Adoption costs can depend in part on subsidies that the government offers for battery investments in year y . We consider subsidy paths that evolve deterministically and are known to market participants.

Besides costs, agents must also forecast the expected current and future revenues from their system. The annual per-unit revenues depend on both the year and the aggregate capacity of storage present in the market. The year matters both because the expansion of renewable energy generation over time will likely increase the value of storage by increasing intertemporal price fluctuations and also because the year may affect available subsidies. Following California's renewable portfolio standard, we model renewable energy market share as the exogenous and deterministic function of y shown in Figure A.2. Aggregate storage capacity matters because of equilibrium effects: with additional capacity, storage owners will arbitrage away more of the intertemporal price differentials, reducing per-unit revenues.

Define K to be the aggregate battery capacity present in the market at the start of a year. The agent's state includes the aggregate state, (c, y, K) , plus its capacity, which starts at $k = 1$ upon installation. Define $K^*(c, y, K)$ to be the equilibrium aggregate storage capacity following adoption at state (c, y, K) ; K^* includes the existing capacity K plus the capacity from the new adopters. Given the rational expectations assumption, agents can accurately predict K^* given (c, y, K) .

Owners of storage capacity buy and sell energy to maximize expected discounted profits in every small time interval of each year. Define $\pi(y, K)$ to be the expected revenues per unit of capacity from storage at year y with capacity K and $\delta(y, K)$ to be the capacity depreciation rate.¹³ Thus, a battery owner that installs a battery system at state (c, y, K) will have $\delta(y, K^*(c, y, K))$ of capacity at year $y + 1$. We microfound $\pi(y, K)$ and $\delta(y, K)$ from our operations model, as we discuss in Section 3.2.

¹³ $\pi(y, K)$ and $\delta(y, K)$ incorporate the fact that agents will modulate usage of their battery to lower depreciation. We discuss this point further in Sections 3.2 and 4.2.

We describe the agent's decision problem with the following Bellman equation:

$$\begin{aligned}
\mathcal{V}(k, c, y, K) &= \mathbb{1}\{k = 0\} \\
&\left[\max \left\{ \overbrace{\pi(y, K^*) - c + \beta \int \mathcal{V}(\delta(y, K^*), c', y + 1, \delta(y, K^*) K^*) dG^{c'}(c'|c, y)}^{\text{Value from adopting}}, \right. \right. \\
&\left. \left. \overbrace{\beta \int \mathcal{V}(0, c', y + 1, \delta(y, K^*) K^*) dG^{c'}(c'|c, y)}^{\text{Value from waiting}} \right\} \right] \\
&+ \mathbb{1}\{k > 0\} \left[\underbrace{\pi(y, K^*)k + \beta \int \mathcal{V}(\delta(y, K^*) k, c', y + 1, \delta(y, K^*) K^*) dG^{c'}(c'|c, y)}_{\text{Value if adoption before } y} \right], \tag{1}
\end{aligned}$$

where integration is over the conditional density of the next period's costs net of subsidies, $dG^{c'}(c'|c, y)$ (and where K^* abbreviates $K^*(c, y, K)$ throughout).

In (1), an agent that has not already adopted can invest (the second line) or wait (the third line). These agents face an important trade-off in their capacity investment problem. On the one hand, agents that do not invest maintain the option to invest in future years with lower capital costs (unless subsidies expire). On the other hand, agents that wait and do not invest forgo $\pi(y, K^*)$. Finally, agents that already invested (the fourth line) face no further choices, but their capacity depreciates over time.

Equilibrium of Model

A market equilibrium consists of values of K^* for all values of the aggregate state such that no potential adopters want to deviate from their strategy given K^* . The equilibrium condition specifies that potential entrants must be indifferent between adopting and not adopting for all states with positive investment:

$$\begin{aligned}
&\overbrace{\pi(y, K^*) - c + \beta \int \mathcal{V}(\delta(y, K^*), c', y + 1, K^* \delta(y, K^*)) dG^{c'}(c'|c, y)}^{\text{Value from adopting}} \\
&= \underbrace{\beta \int \mathcal{V}(0, c', y + 1, K^* \delta(y, K^*)) dG^{c'}(c'|c, y)}_{\text{Value from waiting}}, \quad \forall c, y, K \text{ s.t. } K^* > K. \tag{2}
\end{aligned}$$

In addition, for all states with zero investment, $K^* = K$, and the value from adopting must be less than or equal to the value from waiting.

We solve for the competitive dynamic equilibrium by computing the social planner's problem, which is easier to compute since it does not require that an equilibrium condition such as (2) hold (Ljungqvist and Sargent, 2012; Lucas and Prescott, 1971). Define $GSS(y, K)$ to be the social surplus from the electricity market at year y with capacity K minus the surplus in the market without any battery capacity, gross of battery capital costs.¹⁴ We then express the planner Bellman equation as:

$$\mathcal{W}(c, y, K) = \max_{K^* \geq K} (3) \left\{ K^* GSS(y, K^*) - c(K^* - K) + \beta \int \mathcal{W}(c', y + 1, \delta(y, K^*) K^*) dG^{c'}(c' | c, y) \right\}.$$

Comparing (3) to (1), the planner faces incentives on its last unit of investment that are equivalent to the agents in the competitive equilibrium. We compute (3) by discretizing both c and K . We choose a range for these values that is sufficiently broad to avoid constraining the solution during the time period we study.

3.2 Operations Model

Our operations model and our linking regression allow us to obtain $GSS(y, K^*)$ and $\delta(y, K^*)$ for a range of values of y and K^* . Since our data contain essentially no variation in battery capacity, we calculate $GSS(y, K^*)$ and $\delta(y, K^*)$ across different values of K^* as counterfactuals from a dynamic competitive equilibrium operations model. We then use the in-sample variation in renewable energy production to project these quantities to future years with more renewables.

In the operations model, battery operators, or agents, buy and sell energy in the real-time electricity market in every five-minute time interval, with the goal of maximizing their expected discounted profits from being arbitrageurs. We model agents as solving infinite-horizon dynamic problems where the structural parameters for each day are repeated in perpetuity. We believe that this is a reasonable approximation because we focus on batteries that can completely fill or empty within a few hours, so expectations about changes in future days' demand and supply conditions will have

¹⁴We discuss our microfounding of $GSS(y, K)$ in Section 3.2 below.

relatively little influence on charging decisions.

Each agent’s charge decision at each time interval is a function of its charge level and the market state, which characterizes the current and expected future electricity market prices. Although each agent takes electricity prices as given, it knows that battery operations together will affect dispatchable generator production levels and through this affect equilibrium marginal costs and prices. We estimate marginal cost curves for dispatchable generators that account for ramping costs, by letting marginal costs depend on lagged production.

Storage Technology

Our modeling approach captures three critical properties about battery storage technology. First, a battery’s power capacity F determines what fraction of the battery can be charged or discharged in each five-minute interval and therefore how *quickly* the battery can transition from full to empty and vice versa. Second, we model the round-trip efficiency of the battery, v , which is the percentage of energy that is lost during a charge/discharge cycle. Following Section 2.2, we model four-hour batteries and thus set $F = \frac{1}{4 \times 12}$, and $v^2 = 0.85$.

Finally, we model capacity fading or depreciation, which occurs when a battery’s energy capacity decreases with repeated use. Lithium-ion batteries, as well as most other batteries, will exhibit substantial depreciation. A storage operator may not want to engage in arbitrage if the expected profits are not substantial enough to justify the additional depreciation from the arbitrage. We model capacity depreciation using [Xu et al. \(2016\)](#). It would be computationally difficult to model agent’s optimization over depreciation in the operations model. Instead, as we detail in Section 4.2, we account for capacity depreciation with a heuristic optimization process.

Agent Decision Problem and Equilibrium of Model

At each five-minute time interval, each agent makes charge/discharge decisions in order to maximize the sum of its expected discounted profits. We let S denote the number of time intervals within a day (i.e., $S = 288$), D denote the number of days within a year, d denote any day in our (multi-year) sample, and s denote a particular time period. The per-period discount factor is then $\beta^{\frac{1}{SD}}$.

We focus on a symmetric equilibrium, where all battery operators start each period with the same fraction already charged—which we denote $f \in [0, 1]$ —and then choose the same charge/discharge fraction each period—which we denote q . Let $Q(q)$ be the quantity of electricity supplied to the grid by battery operators at a period where this (common) discharge fraction is given by q :

$$Q(q) = K^* \times \left(\mathbb{1}\{q > 0\}qv + \mathbb{1}\{q < 0\}q/v \right).$$

We model the *net load*—the electricity demanded by final users net of the amount produced by intermittent renewable sources—as an autoregressive process whose mean depends on the time of day, s . Define X to be the net load and Z the amount of electricity that needs to be supplied by dispatchable generators, at some state. We assume that $X = X_s^L + \varepsilon^L$, where X_s^L is the interval-of-day mean of net load and ε^L is the deviation of the realization of net load from the interval-of-day mean. In the absence of storage, $Z = X$, since net load is the amount of electricity that needs to be supplied by dispatchable generators. With battery storage, $Z = X - Q(q)$.

The wholesale market price and marginal cost of production are a function of s , Z , last period's Z , which we denote \tilde{Z} , and ε^P :

$$P(s, Z, \tilde{Z}, \varepsilon^P) = MC(s, Z, \tilde{Z}, \varepsilon^P), \quad (4)$$

where $MC(s, Z, \tilde{Z}, \varepsilon^P)$ is the marginal cost function, and is equal to price by our perfect competition assumption. We include \tilde{Z} to allow for ramping costs. The ε^P term represents other factors that determine the price of electricity conditional on the amount of electricity supplied, and includes factors such as weather, generator outages, and transmission congestion. We assume that the residuals ε^L and ε^P have a joint conditional distribution $dG^\varepsilon(\cdot, \cdot | \cdot, \cdot)$. The current values of ε^L and ε^P and their joint conditional distribution is known to the agents.

While equation (4) specifies that price is equal to marginal costs, one can also interpret our approach as recovering a more general supply relationship for the set of existing generators, which themselves might have market power. In this case, the supply relationship may even include oligopoly power. Thus, our framework is appropriate for analyzing the market impacts of a small battery fleet, even in the presence

of dispatchable generator market power. However, in the case that the generators and batteries are in oligopolistic competition, the counterfactual presence of a large battery fleet may affect equilibrium behavior of generators in a way that could deviate from the supply relationship we estimate. Even in this case, our results could be consistent with a model where battery operators first choose quantity levels and generators then choose their strategies under oligopolistic competition, if generators were static players. However, the ramping costs in our model imply that both the generators and battery operators are dynamic agents. For this reason, the state-contingent production responses of this oligopoly may change following large-scale battery adoption due to the storage operators' decisions affecting the future state-contingent price distribution. Therefore, the supply relationship may be different from what we estimate with large-scale battery adoption, generator oligopoly power, and ramping costs.

We can write the agent optimization problem under the symmetric equilibrium as:

$$\begin{aligned} & \mathcal{V}^d(f, s, \tilde{Z}, \varepsilon^L, \varepsilon^P) = \\ & \max_q \left\{ P(s, Z, \tilde{Z}, \varepsilon^P) \times (\mathbb{1}\{q > 0\}qv + \mathbb{1}\{q < 0\}q/v) \right. \\ & \left. + \beta^{\frac{1}{\bar{s}D}} \int \mathcal{V}^d(f - q, s + 1 - \mathbb{1}\{s = S\}S, Z, \varepsilon^{L'}, \varepsilon^{P'}) dG^{\varepsilon'}(\varepsilon^{L'}, \varepsilon^{P'} | \varepsilon^L, \varepsilon^P) \right\}, \quad (5) \\ \text{s.t. } & Z = X_s^L - Q(q^*(f, s, \tilde{Z}, \varepsilon^L, \varepsilon^P)) + \varepsilon^L, -Fv \leq q \leq F/v, \text{ and } 0 \leq f - q \leq 1. \end{aligned}$$

where ε' denotes the value of ε next period, and where $q^*(f, s, \tilde{Z}, \varepsilon^L, \varepsilon^P)$ is the equilibrium quantity discharged at that state and is equal to the value of q that maximizes (5) at every state.

Analogously to our approach for solving the equilibrium in the investment stage, we recast the battery operations problem as a social planner's problem. For a similar model to ours, [Cullen and Reynolds \(2017\)](#) prove that competitive equilibria and a solution to the planner's problem exist, and that that the planner's solution is equivalent to all competitive equilibria. We rewrite the problem as the single-agent planner's problem whose allocation is then equivalent to the competitive equilibrium problem. The objective of the social planner is to maximize welfare. Since we assume that electricity demand is perfectly inelastic in the short-run, the planner will meet demand by choosing the state-contingent battery discharge fraction $q^*(f, s, \tilde{Z}, \varepsilon^L, \varepsilon^P)$ that minimizes the total expected discounted cost of electricity production.

Let $TC(q, s, \tilde{Z}, \varepsilon^L, \varepsilon^P)$ denote the period total cost of production for any state. It is equal to fixed costs plus the integral of marginal cost from zero to the amount of dispatchable generation. It would be difficult to identify the impact of \tilde{Z} on fixed costs using marginal cost (or equivalently in our context, price) data alone. Accordingly, while we allow \tilde{Z} to affect period marginal costs, we assume that it cannot affect period fixed costs. Any remaining fixed costs (e.g., capital costs or annual maintenance costs) are not relevant to the planner decision, since dispatchable generation capacity is fixed. Hence, we assume that fixed costs are 0 and write:

$$TC(q, s, \tilde{Z}, \varepsilon^L, \varepsilon^P) = \int_0^{X_s^L - Q(q) + \varepsilon^L} P(s, \zeta, \tilde{Z}, \varepsilon^P) d\zeta. \quad (6)$$

We then write the social planner's Bellman equation as:

$$\begin{aligned} \mathcal{W}^d(f, s, \tilde{Z}, \varepsilon^L, \varepsilon^P) = \max_q \left\{ -TC(q, s, \tilde{Z}, \varepsilon^L, \varepsilon^P) \right. \\ \left. + \beta^{\frac{1}{\bar{s}D}} \int \mathcal{W}^d(f - q, s + 1 - \mathbb{1}\{s = S\}S, Z, \varepsilon^{L'}, \varepsilon^{P'}) dG^{\varepsilon'}(\varepsilon^{L'}, \varepsilon^{P'} | \varepsilon^L, \varepsilon^P) \right\}, \quad (7) \\ \text{s.t. } Z = X_s^L - Q(q) + \varepsilon^L, -Fv \leq q \leq F/v, \text{ and } 0 \leq f + q \leq 1. \end{aligned}$$

We solve the operations model by discretizing the state elements \tilde{Z} , ε^L , ε^P , and f into 10 dimensions each and solving the social planner's problem.¹⁵ We solve the optimization separately for each day in our 4-year main estimation sample and across 8 candidate values of K^* . These dimensions result in an overall size of the state space that is roughly $10 \times 10 \times 10 \times 10 \times 288 \times 4 \times 365 \times 8 \approx 33$ million states. We solve the optimization independently for each day- K^* pair which results in about 11,000 dynamic problems with 2,880,000 states each.¹⁶ The infinite horizon solution is very computationally challenging to solve. We instead solve for a finite approximation of the infinite horizon model. For each day, we set up a finite horizon model with the base 288 periods for the day plus 288×3 additional periods which repeat the same set of net load and marginal cost parameters as the base periods. We then kept the policies

¹⁵We discretize the transitions of $\varepsilon^L, \varepsilon^P$ by assuming that the innovation to these shocks are independent and normally distributed. We use the Rouwenhurst method to discretize ε^L , which avoid the sensitivity of the [Tauchen \(1986\)](#) procedure to very persistent processes ([Kopecky and Suen, 2010](#)).

¹⁶We also solve the operations model under an (infeasible) assumption of perfect foresight. For this model, we assume that the current and future values of $\varepsilon^L, \varepsilon^P$ are known to the agent before it makes its operations decisions. The state space for this model is thus much smaller.

for the first 288 periods and used these to compute $GSS(y, K^*)$, as we discuss in Section 4.2 below. We verified that the policies computed from the finite approximation are virtually identical to the policies from the infinite horizon solution.

4 Estimation

This section first discusses our estimation of the inputs to the operations model. We then discuss our estimation of the regressions that links the two models. Finally, we discuss our estimation of the inputs to the adoption model.

4.1 Estimation of Inputs to the Operations Model

Computation of our operations model requires an estimation of the structural parameters underlying net load and the electricity marginal cost curve. We estimate our model using both CAISO’s day-ahead and real-time wholesale electricity markets. Specifically, we use forecasts of (hourly) net load and prices from the DAM to estimate our structural parameters underlying $P(\cdot, \cdot, \cdot, \cdot)$ and X^L , as this information would be feasible to battery operators. We then use 5-minute realizations from the RTM to obtain the distribution and values of ε at each time period. This approach allows us to account for the high frequency changes in market conditions over time.

Net Load

We assume that net load for electricity is perfectly inelastic and hence does not respond to price variations. The process for net load (X_t^L) at any five-minute period in our sample, t , is given by the following equation:

$$X_t^L = \underbrace{E_0 [X_t^L]}_{X_{s(t)}^L} + \underbrace{[X_t^L - E_0 [X_t^L]]}_{\varepsilon_t^L}, \quad (8)$$

where $E_0[\cdot]$ is the expectation taken at time “zero,” $s(t)$ is the interval of day corresponding to t , and ε_t^L represents the deviation in net load from what was expected in the day-ahead market.

In (8), we obtain $X_{s(t)}^L$ from the net load forecast published by the system opera-

tor in the DAM, and X_t^L from the RTM.¹⁷ Since the DAM net load forecasts are only reported at the hourly frequency, while our operations model is formulated at the five-minute frequency, we temporally disaggregate the DAM net load forecasts using a Kalman filter/smoothing approach; see Online Appendix B for details.

We model the transition of ε^L as an AR(1) process given by:

$$\varepsilon_t^L = \rho^L \varepsilon_{t-1}^L + \eta_t^L, \quad \eta_t^L \sim N(0, \sigma_L), \quad (9)$$

where ρ^L and σ_L are parameters to estimate. We estimate the AR(1) model using ordinary least squares (OLS) on ε^L estimated from a training sample in 2015,¹⁸ and hold these parameters fixed over the evaluation sample, 2016–19, which we then use to compute the value of batteries. This ensures that the model would be feasible to estimate and implement given the information set of a market participant.

Table A.1 in Online Appendix A summarizes estimation results for the model of net load. The day-ahead forecasts of net load are relatively accurate.¹⁹ Our estimate of ρ^L is very close to one—indicating a high level of persistence in the day-ahead forecast errors. The parameters governing the AR(1) process (ρ^L, σ_L) are fairly stable across both our training (i.e., 2015) and evaluation samples (i.e., 2016–19), with only σ_L appearing to exhibit a modest increase over the evaluation sample (Table A.1, panel b).

Marginal Cost Curve

We adapt the functional form for marginal cost from the literature on commodity storage. Following Pirrong (2012), we express price as a function of electricity supplied Z given available generation capacity \mathcal{K} :

$$P(Z|\mathcal{K}) = \theta_1 + \theta_2[\mathcal{K} - Z]^{-\theta_3}, \quad (10)$$

¹⁷We measure X_t^L as the amount of energy supplied in MWh per 5-minute interval.

¹⁸Day ahead forecasts for solar and wind are publicly available starting in Nov. 2015. Thus, our training sample includes only data from Nov. and Dec. 2015.

¹⁹CAISO market reports indicate that the CAISO day-ahead load forecasts are shaded up to ensure sufficient supply is available. We scale the net load forecasts by 0.95 to reflect this practice. This choice is supported by the empirical relationship between the day-ahead market forecasts and the realized values, see Table A.1, panel (a) in Online Appendix A.

where $\theta \equiv (\theta_1, \theta_2, \theta_3)$ are parameters that we estimate and that vary at the daily level. The functional form in (10) has two appealing properties for our application. First, as long as $\theta_2, \theta_3 > 0$, P is monotonically increasing in Z , which is critical for solving the operations model. Second, it is parsimonious, yet flexible enough to capture the highly convex shape of the electricity marginal cost curve. In particular, price rises indefinitely as Z approaches \mathcal{K} . Thus, this functional form can capture the high price spikes that occur frequently in the real-time market.

In (10), \mathcal{K} indicates the generation capacity that is available to produce at any given time. In principle, available capacity includes generators that are currently online or those that can quickly become operational without any lead time to start up (e.g., gas peaker plants). For the final price—RTM price—we specify:

$$\begin{aligned} \mathcal{K} &= \kappa^\alpha \tilde{Z}^{1-\alpha} \exp(\varepsilon^P) & (11) \\ \Rightarrow P^{RTM}(Z|\mathcal{K}, \theta, \alpha) &= \theta_1 + \theta_2 \left[\kappa^\alpha \tilde{Z}^{1-\alpha} \exp(\varepsilon^P) - Z \right]^{-\theta_3}, \end{aligned}$$

where κ and α are two additional parameters to estimate, that also vary at the daily level. Our functional form for \mathcal{K} is Cobb-Douglas in a constant κ , lagged generation \tilde{Z} , and an unobservable term ε^P . By including \tilde{Z} in (11), we are able to capture ramping costs: if electricity supplied last period is higher, this will raise the current available capacity, which will raise the quantity at which prices start to spike in the current period. The α parameter governs the relative importance of \tilde{Z} versus κ in determining the available generation capacity. For $\alpha = 1$, marginal cost is static and there are no ramping costs, while if $\alpha < 1$, an increase in generation last period will reduce marginal costs in the current period.

We include the unobservable ε^P as an idiosyncratic shock to \mathcal{K} in determining P^{RTM} , which allows for shifts in RTM electricity supply to be due to unforeseen changes in available generation capacity. This non-linear entry of ε^P into P^{RTM} allows for extreme price spikes (drops) to be mitigated by storage operators discharging (charging) energy. We believe that this placement of the structural residual generates more plausible counterfactuals than would an additive structural unobservable on P^{RTM} .

We use DAM prices and quantities to estimate the marginal cost curves, because these data are available prior to the operating day, and therefore, could feasibly be

used by battery operators in developing output choices in the RTM. Our model of DAM price is similar to P^{RTM} but with the exclusion of ε^P , which we assume to be realized in the 24+ hour period after the DAM clears. We also allow for the possibility of measurement error and other linear disturbances and write:

$$E \left[P^{DAM}(Z|\tilde{Z}, \theta, \kappa, \alpha) \right] = \theta_1 + \theta_2 \left[\kappa^\alpha \tilde{Z}^{1-\alpha} - Z \right]^{-\theta_3}. \quad (12)$$

We estimate the marginal cost curve parameters (θ, κ, α) separately for each day of our sample using non-linear least squares. Specifically, for each day d , our estimates satisfy:

$$\hat{\theta}^d, \hat{\kappa}^d, \hat{\alpha}^d = \arg \min_{\theta, \kappa, \alpha \in \Theta} \sum_{t \in \mathcal{D}(d)} \left[P_t^{DAM} - \left(\theta_1 + \theta_2 \left[\kappa^\alpha X_{s(t-12)}^{L, 1-\alpha} - X_{s(t)}^L \right]^{-\theta_3} \right) \right]^2, \quad (13)$$

where $\mathcal{D}(d)$ comprises the time periods belonging to day d , and Θ describes the allowable domain for the marginal cost parameters. Given the hourly frequency of the day-ahead market, these (daily) non-linear least squares regressions constitute regressions with 24 observations each.²⁰ Because $Q_t \approx 0$ for most of our sample, we use X instead of Z in estimating (13).

We estimate an AR(1) model using OLS on the realizations of ε_t^P for a training sample of Nov. and Dec. 2015 and fix these parameters over our evaluation sample. As was the case for net load, our approach of estimating these parameters from a training sample ensures that the model would be feasible to estimate given the information set of a battery operating in the real-time market. Online Appendix C provides more discussion on our estimation of electricity generation costs.

4.2 Regressions Linking the Operations and Adoption Models

We use the dynamic competitive equilibrium policies from our storage model to estimate surfaces of $GSS(y, K)$ and $\delta(y, K)$, which we then use in our adoption model. Our basic approach is to calculate optimal policies from the operations models and then compute GSS and δ using these policies. Let $q^*(f, s, \tilde{Z}, \varepsilon^L, \varepsilon^P|d, K)$ denote the policy consistent with the maximization process in (7) at day d and with capital K .

²⁰For this reason, the lagged value of net load in the non-linear least squares step constitutes the lag of mean net load last hour, $X_{s(t-12)}^L$.

We estimate q^* for each day in our 2016–19 sample and for a grid of eight candidate values of K ranging from 10 MWh to 50,000 MWh. These values then form the basis points for our estimation of the surfaces.

For each value of K and each week in our sample, we simulate GSS over a week-long period where batteries start with 50% charge.²¹ At each five minute period, our simulation uses the calculated policies q^* , evaluated at the observed values of the deterministic states s, d, K ; the realized values of the residuals $\varepsilon^L, \varepsilon^P$; and at the state variables f, \tilde{Z} consistent with previous actions.²² The simulation then outputs the realized GSS from having battery operators with capacity K for each week.

We use a simulation approach to calculating the value since we compute the value function using a finite approximation, which gives accurate policies, though not accurate values. This approach also is robust to misspecification in the distribution assumptions around ε^L and ε^P . Finally, it allows us to use a heuristic approach to incorporate capacity fading, as we discuss below.

We use our approximation to GSS to estimate the following regression:

$$\begin{aligned} \frac{GSS_{wk}}{K_k} = & \gamma_1 \ln(K_k) + \gamma_2 \text{RenewableShare}_w + \gamma_3 \ln(K_k) \times \text{RenewableShare}_w \\ & + \gamma_4 X_w + \nu_w + \varepsilon_{wk}, \end{aligned} \quad (14)$$

where w indexes sample week, k indexes sample capacity levels, K_k is a capacity in our sample, RenewableShare_w is the share of load generated by renewables in the week, X_w are other controls, ν_w is a week-of-year fixed effect, and ε_{wk} is an i.i.d. unobservable. The fitted values from (14) provide us with GSS at a weekly level across K^* values and years in our sample.²³

Note that $\text{RenewableShare}_{wk}$ fluctuates seasonally, but is increasing over time on average. As a consequence, this variable could be correlated with other factors that are changing over time or are seasonal and that might affect the social value of storage. To address these endogeneity concerns, we include week-of-year fixed effects, ν_w . We also control for the average price of natural gas in week w , and the average

²¹Because we define simulated realized profits at the week level, our sample starts on Friday, Jan. 1, 2016 and ends on Thursday, Dec. 27, 2019.

²²We set \tilde{Z} for the first five-minute interval of the week to the value that is consistent with no charge or discharge.

²³We transformed GSS from a weekly to an annual measure to use it in our adoption model.

peak electricity load (demand) in week w . Last, we control for the Sacramento Valley water-year index in week w , which proxies for the amount of hydroelectric resources available during each week. In contrast, $\ln(K_k)$ will not be correlated with any omitted variables because we use the same set of candidate battery capacity values to solve the model in every distinct week of the sample.

Accounting for Battery Capacity Depreciation

We use heuristic methods to account for how agents would change their operations and adoption behavior to account for the fact that battery capacity will depreciate through use. The idea is that the perception of a lower-than-actual round-trip efficiency will make a battery operator more reluctant to charge or discharge unless the payoff is sufficiently high. This may then help the battery operator in its expected long-run profits by causing less capacity depreciation. Thus, we use a perceived lower-than-actual round-trip efficiency to proxy for long-run capacity depreciation. This approach is feasible for the agent to implement and ensures we do not overstate the value of storage by ignoring depreciation.

We operationalize this idea by again splitting our sample into a training sample, 2015, and an evaluation sample, 2016–19. We solve the operations model for the training sample using a sparse grid of different candidate perceived efficiency levels $[\cdot 7v, \cdot 75v, \dots, v]$.²⁴ For each candidate perceived efficiency and value of K , we use our training sample to solve for optimal policies, simulate the evolution of the state-of-charge, f , using the actual demand and price data, and then feed the simulated state-of-charge series into an engineering capacity depreciation model. See Online Appendix D for details. For each case, the capacity depreciation model outputs δ , the percent by which the effective battery capacity depreciates over the training sample. For each K , we calculate the best perceived efficiency level as the one that maximizes an approximation to expected future value, $\frac{GSS}{1-\beta-\delta}$ over the training sample.

Using our estimated optimal heuristic policy, we obtain an estimate of δ for each week in our evaluation sample and K . We then calculate a regression that is identical in sample and regressors to (14), but with δ_{wk} instead of GSS_{wk}/K_k as the dependent variable. We use the fitted values from this regression to calculate an annualized

²⁴We solve the perfect foresight version of these models, because of computational ease and because DAM forecasts of net load (load net of renewable generation) were not available before November 2015.

$\delta(y, K^*)$, which enters into the adoption model (3). We also use our calculated δ values to approximate the expected future value of a battery during our evaluation sample, again with the formula $\frac{GSS}{1-\beta-\delta}$.

4.3 Estimation of Inputs to Adoption Model

To solve the adoption model, we estimate the evolution of battery capital costs over time. We specify the following unit root with drift process for the cost of the storage technology, c_y :

$$c_y = c_{y-1} \exp(\tau) \exp(\xi_y), \quad \xi_y \sim N(0, \sigma_c^2), \quad (15)$$

with c_{2018} as the capital cost of batteries in 2018, the initial year, and τ and σ_c governing the size of the drift and future uncertainty of costs. To the extent that $\tau < 0$, the costs of storage will trend down over time on average. The uncertainty about the size of these future declines in costs is captured by the process ξ_y . We assume that ξ_y are i.i.d. over time.

The National Renewable Energy Laboratory (NREL) cost projections in Figure 2a motivate this functional form. In particular, they demonstrate: (i) a downward trend in costs, (ii) a non-linear trajectory to costs, (iii) an increase in the uncertainty the further we are in the future, and (iv) positive skewness in the distribution of future costs. These patterns motivate our modeling approach in (15): The downward trend in costs motivates the drift term in our model; the non-linear trajectory motivates the exponential formulation; the increasing level of uncertainty in the forecast uncertainty motivates the unit-root (in logarithms) formulation of the model; and the positive skewness in the cost assessments justifies the log-normal distribution for the shock process.

We estimate two parameters in (15): the magnitude of the downward drift (τ) and the size of the shock process governing the level of cost uncertainty (σ_c). Importantly, we do not observe actual realizations of the battery capital cost process, only the set of *projected* cost realizations from Cole and Frazier (2019). Therefore, our estimation treats each cost projection (i.e., each line in Figure 2a) as a realization of the cost process. We use a method of moments approach to recover τ and σ_c . Online Appendix E derives the moment conditions for estimation. Our estimates for the cost process are $\hat{\tau} = -0.044$ (with a standard error of 0.001) and $\hat{\sigma}_c = 0.064$ (with a standard error of 0.003). Following Cole and Frazier (2019), our simulations use an initial condition for

capital costs in 2018 of $c_{2018}=\$380/\text{kWh}$.

5 Results

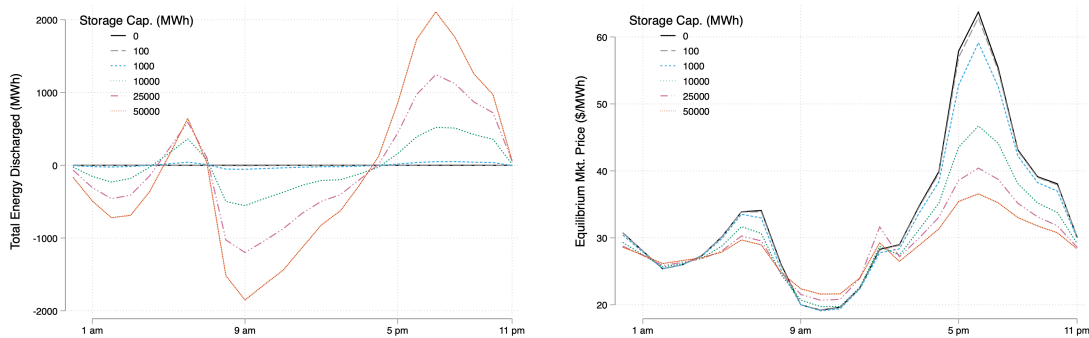
This section discusses results from our operations model, our linking regressions, and our adoption model. It then provides an overall discussion and analysis of public policies.

5.1 Operations Model Results

Figure 3a illustrates the mean simulated battery discharge quantity for each hour of the day for our evaluation sample, 2016–19. Each line in the figure shows battery output for a specific aggregate battery fleet capacity K . Batteries discharge the most during the hours that net load is the highest—the evening peak hours of 5–10 pm, but also discharge on average between 5–7 am. As aggregate battery capacity grows, total discharges increase in the evening and total charges increase during the day.

Figure 3b shows that, as the fleet expands, battery operations exert a strong effect on lowering the volatility of mean equilibrium prices. It illustrates that battery operations have the biggest impact on prices during the peak evening hours, and have a relatively small effect on prices during the middle of the day, because marginal costs

Figure 3: Mean Battery Output and Equilibrium Prices Effects



(a) Mean Hourly Battery Output Across Day

(b) Mean Hourly Equilibrium Prices

Notes: Each line plots the mean counterfactual outcome across all days during 2016–19.

are relatively low and flat during these hours.²⁵ Additionally, Figure 3b shows that the first few units of battery investment would have the largest impact on equilibrium price, whereas incremental storage investment has a smaller impact on prices. The first batteries that enter the market will reduce the occurrence of extreme pricing events by discharging during periods when net load approaches the available generation capacity. By doing so, the batteries will reduce prices and also move the equilibrium to flatter regions of the marginal cost curve, thus reducing the marginal impact of subsequent battery entry on prices.

Table A.4 in Online Appendix A emphasizes this result. It shows that the first 1,000 MWh of storage capacity would reduce evening prices by 6% (\$54.27/MWh to \$51.15/MWh) and overall average price by over 3% (\$35.97 per MWh to \$34.79 per MWh). In contrast, an increase in capacity from 25,000 to 50,000 would only reduce mean prices by an additional 3.2% (\$30.63/MWh to \$29.62/MWh).

Appendix Figure A.5b demonstrates how battery operations would affect the mean generation from dispatchable power plants (e.g., natural gas generators) throughout the day. Unsurprisingly, batteries increase power plant output during the middle of the day and reduce power plant production in the evening peak hours. Notably though, batteries would also change the times of day that dispatchable power plant production troughs and peaks occur. With no battery capacity, the lowest production hour is 11 am, whereas with a large battery fleet the lowest production period moves an hour later to noon. Similarly, the peak for dispatchable production without battery storage is 7 pm, relative to after 8 pm with a large storage fleet. These patterns demonstrate the importance of ramping costs in modeling the equilibrium effects of storage operations. Battery operations can reduce generators' costs by reducing the *rate* that dispatchable production increases. With a large battery fleet, the morning ramp down and evening ramp up are spread over more hours to allow more time for adjustment.

To further understand how large battery fleets would optimally operate, Figure A.6 in Online Appendix A graphs real-time prices and battery operations for two randomly-selected days—June 23rd, 2016 and December 29, 2018—both for a 25,000 MWh capacity. Battery operations change discretely and abruptly during the day. On

²⁵Figure A.5a in Online Appendix A focuses on the evening hours, showing that from 6-7 pm—the hours with the highest average net load—a relatively small 1,000 MWh battery fleet would reduce average prices by over \$10 per MWh.

the left graph, batteries charge substantially in the morning before 8 am, remain idle throughout the middle of the day, and then discharge at different points in time in the evening. On the right graph, where prices did not plummet in the morning, batteries do not charge until later in the day. On both days, batteries reach a full state of charge, wait several hours, and then discharge in the evening when real-time market prices spike. The two days differ in the times at which batteries start charging and discharging. More generally, and consistent with Figure A.6, we find that (1) battery output at any time period varies considerably across days, and (2) on most days, batteries will fully charge prior to the evening ramp-up period and then wait to discharge until a price spike occurs.

As a result of highly volatile real-time prices, battery operational revenues are highly skewed across time periods. From Table A.5 in Online Appendix A, batteries earn over 70% of total revenues during the most profitable 1% of time intervals. For a 1000 MWh battery fleet, each 1 MWh of battery capacity would earn \$37,396 during the most profitable 1% of 5-minute intervals and only \$16,762 across the other 99% of time periods over our sample period. Battery revenues are very sensitive to equilibrium effects. Specifically, battery revenues during the most profitable hours decline dramatically as aggregate battery capacity rises. For example, an increase in the battery fleet from 100 MWh to 10,000 MWh reduces per-unit revenues by nearly 37%. These findings highlight the considerable decreasing returns-to-scale in battery storage capacity, which has important implications for the time path of battery investment.

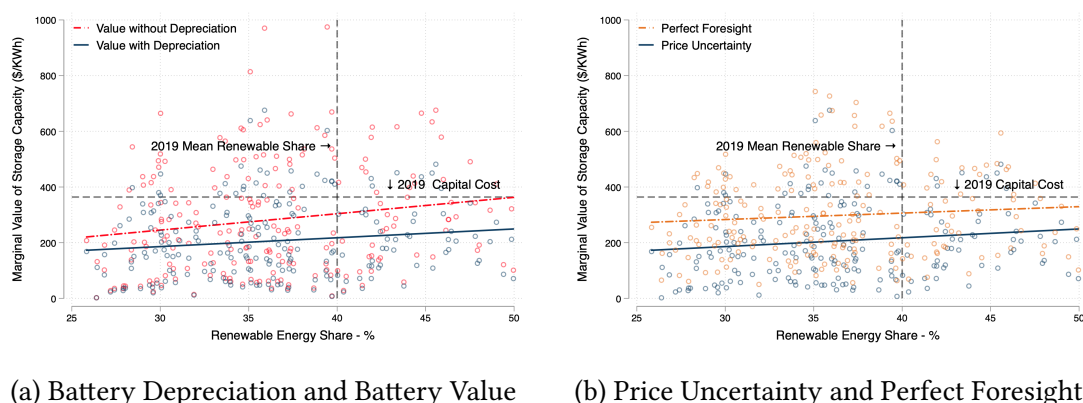
Value of Small Battery Fleet

To understand the value of batteries implied by our operations model, we calculate the gross social surplus from battery storage for each sample week over the 2016–19 period for a small battery fleet of 10 MWh. We convert each of these weekly observations into a “lifetime” value of storage capacity, using an annual discount factor of $\beta = 0.95$.

Figure 4 uses these value calculations to illustrate the value of batteries relative to capital costs. First, Figure 4a plots the marginal social value of storage capacity for each week in our 4-year sample, with and without accounting for depreciation.²⁶ This panel demonstrates a strong positive association between the renewable gener-

²⁶We approximate the marginal value as the average value for this very small fleet.

Figure 4: Renewable Energy, Depreciation, Uncertainty, and the Social Value of Batteries



Notes: Each point in the scatter plots (a-b) represents the marginal value of storage capacity for a single week during the sample (2016–19). The solid lines in (a-b) plot the linear trend for each group. The marginal value is the estimated per-unit value from the first 10 MWh of operational storage capacity. We rescale the estimated weekly storage value into a perpetuity using a 5% annual discount rate and adjusting for the rate of capacity depreciation. All estimates in plot (b) account for battery depreciation from operations.

ation and the value of storage. The dashed-red line plots a simple linear fit of the relationship between marginal storage value and the share of electricity generated by renewable sources, before adjusting for capacity depreciation.²⁷ The dashed-grey line shows expected capital cost per kWh of storage capacity in 2019. Together, these lines show that, absent capacity depreciation, the marginal social value would exceed the 2019 expected capital cost of storage if the renewable energy share were over 50%.

The solid blue line in Figure 4a highlights how capacity depreciation (as discussed in Section 4.2) influences the estimated storage values. Depreciation from cycling reduces the estimated value of storage investment by 24% on average. Moreover, the impact of depreciation is higher with more renewable energy, which is due to batteries cycling more in this case. After accounting for depreciation, the first battery unit would break even in the energy market only when the share of renewable energy was 52% and capital costs declined by 41%, as is expected to occur in 2027.²⁸ This finding emphasizes the significance of accounting for depreciation when measuring the social

²⁷We calculate the renewable energy share as the percentage share of solar plus wind generators during the sample week plus 19%. 19% is the mean share of generation from non-intermittent renewables including hydro, geothermal, and biomass generators across the sample period.

²⁸We calculate the expected renewable share based on the California RPS schedule and expected capital costs based on our capital cost model in Section 4.3.

value of battery capacity.

Figure 4b compares our baseline storage value estimates—that assume battery operators face uncertainty about future wholesale prices—to the value estimates if battery operators have perfect foresight about future load and electricity supply curve realizations.²⁹ Our model with uncertainty, which can be feasibly implemented by battery operators, achieves 68% of the theoretical maximum value under perfect foresight. Although our baseline model under uncertainty attains the majority of the perfect-foresight value, it is notable that the social value of storage could be further increased with a better-performing forecasting model. Importantly, our results that allow for uncertainty should be interpreted as a lower bound for storage value that could be further improved through better forecasting and modeling.

Equilibrium and Distributional Effects of Storage Operations

Table 1 considers the impact of battery fleets of different sizes on overall value and the value to different market participants. From Column 1, a 1,000 MWh storage fleet would increase gross social surplus by \$13.6 million annually.³⁰ A larger fleet with 10,000 MWh would further reduce costs by \$100 million per year. The other columns of Table 1 report how battery operations would affect profits and costs for different market participants. Column 2 indicates that batteries would significantly reduce the total cost (price \times load) that load serving entities need to pay to meet demand. In particular, a 1,000 MWh battery fleet would reduce mean hourly expenditures for utilities by over \$256 million per year. Relatedly, batteries would reduce the revenues of dispatchable generators substantially, by \$227 million per year. Perhaps surprisingly, these battery operations reduce solar and wind generators revenues by \$29 million annually. Although, batteries increase prices between 9 am and 1 pm when solar plants are coming online, batteries also reduce prices during the early afternoon (3-5pm) when many solar generators are still producing. Summing these impacts, solar generators are made slightly worse off by battery operations. These results illustrate that large-scale storage will have important implications on the profits of different industry participants. The reduction in profits to dispatchable generators and solar and wind producers further

²⁹In both cases, we adjust the values to account for depreciation.

³⁰Since we assume that demand is perfectly inelastic, a change in gross social surplus is equal to the change in the total cost of electricity generation.

implies that storage may lead to greater exit or lower investment by these facilities.

Table 1: Annual Gross Social Surplus Across Aggregate Battery Capacity Levels

	Δ Gross Social Surplus	Δ Total Costs to Serve Load	Δ Dispatchable Generator π	Δ Solar and Wind π	Δ Battery π
0	0.00	0.00	0.00	0.00	0.00
100	1.43	-44.10	-39.13	-5.12	1.59
1000	13.58	-256.31	-227.32	-29.60	14.21
10000	99.63	-862.23	-764.47	-80.70	82.68
25000	184.77	-1,157.50	-1,008.45	-87.95	123.83
50000	261.26	-1,377.29	-1,164.05	-102.86	151.06

Notes: All variables are annual means in millions of dollars. “ Δ Gross Social Surplus” is the change in mean total costs of generation relative to the $K = 0$ case. “ Δ Cost to Serve Load” is the change in total price paid by load-serving entities for energy (change in equilibrium price times total load). “ Δ Dispatchable Generator π ”, “ Δ Solar and Wind π ”, and “ Δ Battery π ” are the mean change in annual gross revenues for dispatchable generators, renewable generators, and battery operators respectively.

5.2 Results from Linking Regressions

Table 2 report the results of our linking regressions, which estimate surfaces of $GSS(y, K)/K$ and $\delta(y, K)$. Column 1 shows results from a specification of GSS with logged battery capacity, renewable energy share (wind + solar share), and an interaction term. Column 2, our preferred specification, adds week-level controls for mean load in the evening peak hours, mean natural gas price, and the Sacramento Valley hydroelectric water year index (WYI), and week-of-year fixed effects.

The specifications with and without controls yield very similar results, adding to our confidence that the estimates are not being confounded by electricity market changes that are contemporaneous to renewable energy share changes. In our preferred specification, we estimate a negative and statistically significant coefficient on $\ln(K)$, a positive and significant coefficient on renewable share, and a negative and significant coefficient for the interaction term, consistent with the trends in Figure 4. Overall, our results paint a clear picture of the link between installed battery capacity, renewable generation, and the social value per unit of storage capacity.

The regression estimates indicate that per-unit storage value falls quickly as the aggregate storage capacity in the market rises. This finding is consistent with the significant equilibrium pricing impacts of storage documented in Section 5.1. Moreover,

Table 2: Gross Social Surplus and Discounting by Year and Battery Capacity

	Gross Social Surplus / K (\$/kWh)		Annual Depreciation Rate (%)	
	(1)	(2)	(3)	(4)
ln(K)	-8.220*** (2.702)	-8.220*** (2.748)	0.0089 (0.0075)	0.0089 (0.0076)
Renewable Share (%)	8.485*** (2.577)	8.183* (4.395)	0.0557*** (0.0072)	0.0588*** (0.0091)
ln(K) × Renewable Share (%)	-0.6855*** (0.1625)	-0.6855*** (0.1653)	-0.0028*** (0.0005)	-0.0028*** (0.0005)
Observations	1,664	1,664	1,664	1,664
R ²	0.11863	0.39122	0.21373	0.52397
Within R ²		0.16075		0.17552
Controls + week fixed effects		✓		✓

Notes: In columns 1 and 2, the dependent variable is the present discounted social surplus per kWh of storage capacity, not accounting for capacity depreciation. Each observation represents a single week of the sample for a single storage capacity. In columns 3 and 4, the dependent variable is the annual capacity depreciation due to operations. Columns 2 and 4 include controls for the mean load in the evening peak hours of 5–10 pm over the week, the mean natural gas price over the week, and the Sacramento Valley hydroelectric water year index (WYI) associated with that week. Peak load is the mean load between 5pm and 9pm hours during the week. Standard errors are clustered by week of sample.

the value of storage rises with renewable energy market share, but particularly when there is low storage capacity operating in the market. As aggregate storage capacity increases, the marginal effect of renewable energy additions diminishes because the pre-existing batteries mitigate some of the marginal cost fluctuations that would normally be exacerbated by solar and wind generation.

Table A.6 in Online Appendix A shows that the regression estimates are robust to alternative specifications and control variables. Perhaps the most important control variable is peak load. Changes in electricity demand can strongly impact the value of storage. Table A.6 shows that the results are similar if we control for average load across the entire day instead of at peak times. The results are also similar if we add separate controls for both peak and off-peak load conditions. Last, we estimate a specification that allows for a quadratic term on the renewable share variable. We find that the coefficient on the quadratic term is close to zero and not statistically significant, motivating the use of our linear specification.

Table 2, Columns 3 and 4 show regression results with the annual battery depreciation rate as the dependent variable. The coefficient on the renewable energy share

is positive and statistically significant: as renewable energy increases, the annual depreciation rate also rises because batteries engage in more charge-discharge cycles. Importantly, this finding implies that the marginal effect of increasing renewables on battery value will be smaller after accounting for depreciation. However, the interaction term is negative, which implies that marginal effect of renewable energy on depreciation declines with larger battery fleets.

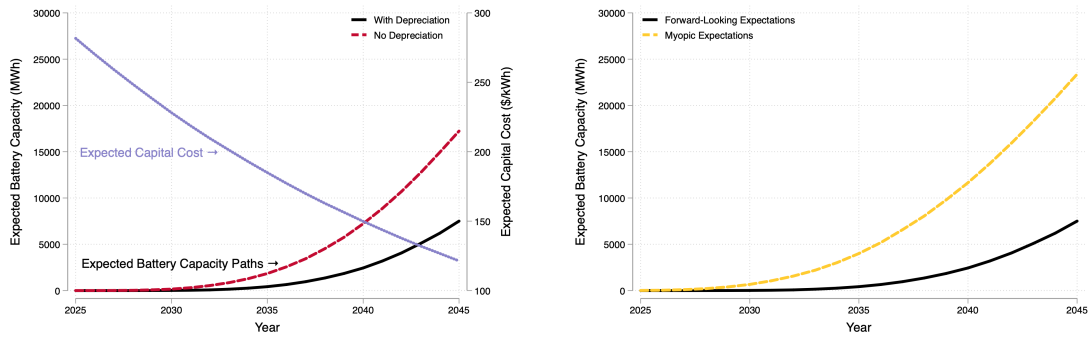
5.3 Battery Adoption Results

The regression estimates outlined above provide the final input needed to solve the adoption model. Figure 5 provides simulated mean competitive equilibrium adoption paths under a variety of alternative assumptions, all using $\beta = 0.95$. The purple line in Figure 5a plots the expected battery capital cost over time implied by our capital cost model outlined in Section 4.3. Throughout each panel of Figure 5, the solid black line shows the expected battery capacity trajectory under our baseline case, in which we assume that: battery capacity depreciates as a function of use; potential adopters have rational expectations over future capital costs; renewable energy increases according to the California RPS; and peak load is held fixed at the 2019 mean level. The solid black line shows that battery adoption begins slowly around 2030 before ramping up and reaching an aggregate capacity 420 MWh in 2035, and 7,500 MWh in 2045.

The remaining lines in Figure 5 explore several potential factors that may be limiting the baseline equilibrium adoption. First, Figure 5a contrasts expected battery capacity over time without capacity depreciation to the baseline. When we ignore depreciation in calculating the value of storage, adoption starts several years sooner and increases at much faster pace. In particular, expected capacity would be four times higher in 2035 (1,840 MWh) and two times larger in 2045 (17,200 MWh).

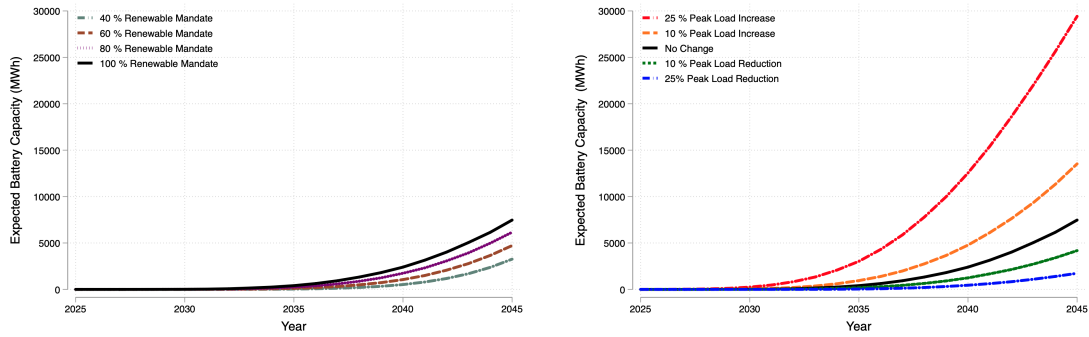
Another factor that encourages potential battery adopters to delay investment is the anticipation of future capital cost reductions. Figure 5b quantifies the influence of future cost expectations on investment by calculating the predicted adoption path for myopic agents. While the forward-looking agents in our baseline know the parameters of the stochastic capital cost process in equation (15), myopic agents assume that the current capital cost will remain unchanged in future years, but are otherwise identical to the baseline agents.

Figure 5: Counterfactual Battery Capacity Adoption Paths



(a) Battery Capacity With vs. Without Depreciation

(b) Myopic vs. Forward-Looking Expectations



(c) Renewable Mandates and Battery Capacity

(d) Peak Demand and Battery Capacity

Notes: In Figure 5a, the purple line shows the expected capital cost over time. In all figures, the solid black line plots expected battery capacity under the baseline case with: capacity depreciation, forward-looking expectations, 100% RPS, and peak load held constant. The other lines plot expected battery capacity adoption under different counterfactuals. Each figure varies a single parameter, and holds all other assumptions fixed.

Myopic agents invest much more heavily in storage between the years of 2025 and 2035. Under myopic expectations, the first unit of battery investment is expected by 2024, with aggregate battery capacity passing 4,000 MWh by 2030, and surpassing 23,300 MWh by 2045. The myopic results are striking, as they indicate that expectations of future battery cost declines may play a big role in limiting adoption.

Another key driver of the battery adoption decisions is the trajectory of future renewable energy generation. Figure 5c measures the effect of changing the renewable portfolio standard on the time path of battery adoption. Specifically, we plot the battery investment path for a 40% RPS by 2045, a 60% RPS by 2045, an 80% RPS by 2045, and a 100% RPS by 2045 (the current policy). With an RPS of 40%—a policy that would hold renewable generation constant at 2019 levels—almost no battery invest-

ment would occur until after 2035, and aggregate storage capacity would remain below 3,300 MWh through 2045. With the more aggressive renewable energy mandates, storage investment substantially increases. The 60% RPS would result in 4,700 MWh of expected storage capacity by 2045, and the 80% RPS would lead to 6,200 MWh by 2045. These results indicate that subsidies will be necessary for battery storage investments to be economically viable in the wholesale energy market unless intermittent renewable penetration is relatively high and/or capital costs decline substantially.

Finally, Figure 5d explores how changes in future electricity load (demand) would change the time-path of battery adoption. In our baseline case, Figure 5a, we assumed that peak load would remain constant at 2019 levels in all future years. However, California's peak load may change over time for a multitude of reasons. On the one hand, peak load could decrease over time due to energy efficiency retrofits and adoption of behind-the-meter storage technologies. On the other hand, rising adoption of electric vehicles could increase peak load if drivers plug in their cars during evening hours. Figure 5d illustrates how different assumptions about future peak load in California would change the trajectory of battery adoption. We evaluate expected battery adoption under five different cases: (1) 25% increase in peak load, (2) 10% increase in peak load, (3) no change in peak load (baseline), (4) 10% decrease in peak load, and (5) 25% decrease in peak load. We find that peak load changes can result in significant changes in expected battery investment. A 25% increase in peak load leads to a massive four-fold increase in capacity by 2045, whereas a 25% decrease in peak load reduces aggregate capacity by 38% relative to the baseline case. These results show that utility-scale battery investment serves as a substitute for other investments that reduce peak load. For instance, energy efficiency retrofits can reduce electricity demand at times of the day when the grid is most strained (Boomhower and Davis, 2020) while home battery installations could also reduce peak household electricity demand. Accordingly, policies that encourage residential storage or energy efficiency investments would reduce the optimal capacity of utility-scale storage investment, while further investments in residential solar might complement them.

5.4 Further Discussion and Policy Implications

Our results analyze the impact and value of battery adoption over time, accounting for complementarity with renewable energy and the equilibrium effects of large-scale battery operations. Taking the California RPS as given, and assuming no battery subsidy or mandate exists, we find that expected battery adoption would begin to increase steadily in the late 2020s. Although storage investment increases substantially after 2030, we find that the overall level of storage investment would likely remain relatively low over the coming decades, reaching 7,500 MWh by 2045. A 7,500 MWh storage fleet composed of 4-hour duration batteries can produce 1,875 MW at any instant, similar to the typical output of a nuclear power plant. While this output would mark a substantial increase relative to present storage penetration, it is only sufficient to serve around 8% of the typical CAISO load.

To better understand why our model predicts relatively low battery adoption, Figure 6a overlays the trajectory of expected capital costs with per-unit value of battery operations over time. We calculate the per-unit value across several candidate capacity levels. For small aggregate battery capacity (e.g., $K = 10$), the gross marginal value of battery operations (i.e., generation cost reductions) increases rapidly over time as more renewables enter the market. Indeed, a 10 MWh battery fleet would be quite profitable by the 2030s. Nevertheless, as more batteries enter the market, the marginal value of additional capacity shifts downward due to market equilibrium effects of operations of the preceding battery stock.³¹ For example, the gross marginal value of storage investment in 2020 falls from over \$200/kWh to \$125/kWh when aggregate capacity increases from 10 kWh to 5,000 kWh. These equilibrium effects prevent a very large storage fleet (e.g., 25,000 MWh) from ever becoming economical unless capital costs were to fall far below current expectations.³²

The battery adoption results have some important implications for policymaking. Specifically, the results suggest that a stringent renewable energy standard alone is not sufficient to encourage enough investment in battery storage for the grid to operate solely using renewable energy and batteries. Consequently, additional policies will

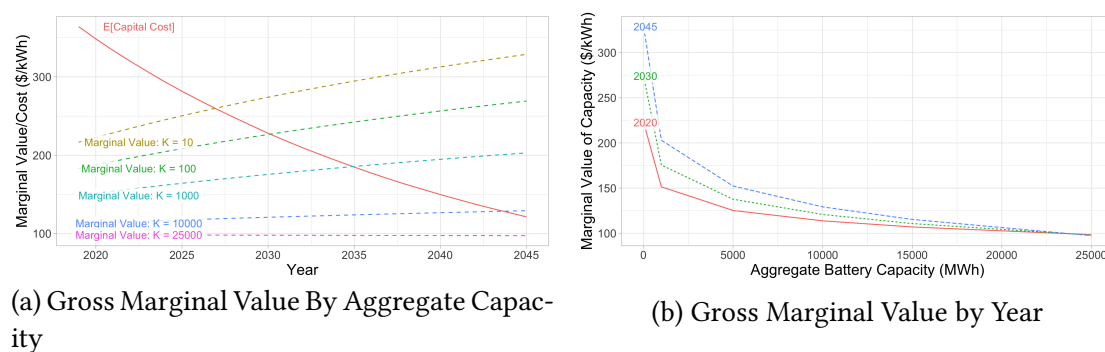
³¹Figure 6b highlights the dramatic decline in gross marginal value as aggregate capacity rises across years with different renewable energy penetration.

³²Note that our analysis holds fossil fuel generation capacity fixed. As more fossil fuel generators retire, this might raise the value of additional battery storage.

likely be needed if policymakers and the public aspire to transform the electric grid to run primarily with intermittent renewable energy in tandem with storage. Policymakers have already begun implementing other rules and regulations to spur investment in battery technologies. For example, several states including California have implemented targets or mandates for battery storage investment. Despite the increasing prevalence of these policies, there is little evidence about their costs or benefits.

To shed light on this issue, we use our adoption model to measure the effect of California’s storage mandate on electricity generation and capital costs. Under the mandate, utilities are directed to procure contracts for storage resources by 2020, and those resources should be fully operational by 2024. Figure 7 shows how various battery mandates—effective by 2024—would change discounted total costs—defined to be the sum of total electricity generation and battery capital costs (i.e., \mathcal{W}). We compare total costs relative to a case with zero battery investment, analogous to a permanent ban on batteries from the electricity market.³³ The black line shows that total cost declines roughly linearly as the level of the battery mandate increases. The y-intercept of the black line, \$925 million, represents the change in total cost under the competitive equilibrium investment path (surplus maximizing investment path) relative to having no battery market.

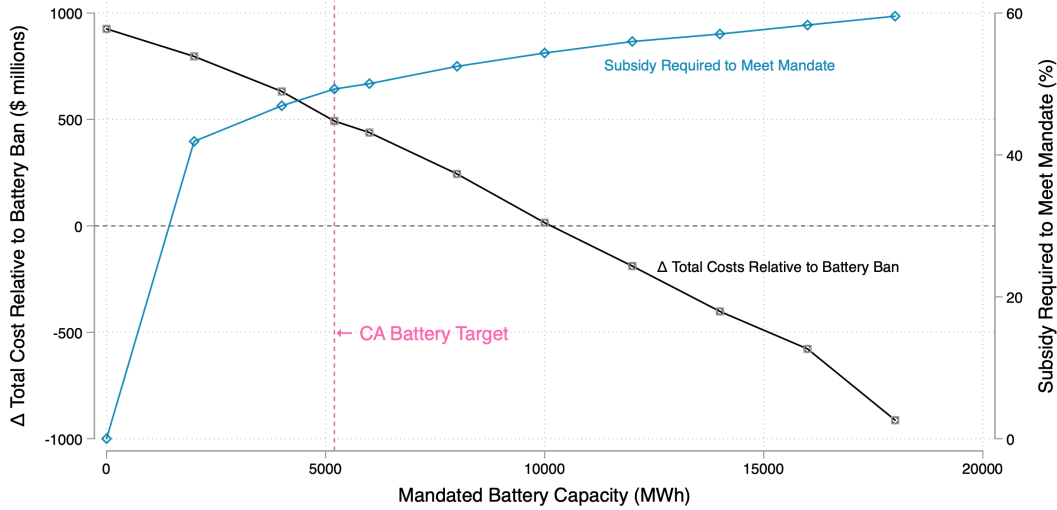
Figure 6: Gross Marginal Value and Cost of Battery Investment Over Time



Notes: In panel (a), the solid red line plots the expected value of future battery capital costs based on the estimated parameters of the cost process. The dashed lines plot the annual value of a battery investment over time, for selected aggregate battery capacity levels. The gross marginal values are obtained by plugging in the associated capacity level and the renewable energy share based on the California RPS into the regressions in Equation 2. Panel (b) shows the relationship between the gross marginal value and aggregate capacity across three selected years, the gross marginal value varies across years due to changes in projected renewable energy share.

³³The assurance that batteries can participate in the wholesale market was guaranteed in 2018 by Federal Energy Regulatory Commission (FERC) Order 841.

Figure 7: Evaluating the Cost of Battery Mandates, Battery Subsidy Policies



Notes: The black line plots the change in discounted total costs (battery capital costs plus generation costs) in millions of dollars as a function of mandated battery capacity, relative to a battery ban (i.e., no battery adoption). We assume the mandated capacity must be achieved by 2024. The pink dashed line indicates the California storage target under AB 2514. The blue line plots the minimum battery subsidy (percentage) required to reach the mandated level.

The vertical pink line in Figure 7 marks the change in total cost imposed by California’s storage mandate.³⁴ We find that the mandate would decrease total costs by \$492 million dollars, or about \$12.45 per California resident, relative to a battery ban. Moreover, any battery mandate below 10,000 MWh would decrease total costs relative to a case where no batteries operate in the wholesale market.

Figure 7 also shows the level of government subsidies for battery storage needed to achieve varying storage targets by 2024. We estimate that California would require a 49% up-front subsidy for batteries to achieve the amount ordered under California’s AB 2514 storage bill. While California’s mandate decreases total costs relative to a ban, it also increases total costs by \$433 million (\$925m-\$492m) compared to the competitive equilibrium investment path.

There are two main channels through which a battery mandate changes total costs relative to the market without a mandate. First, a mandate will decrease total electricity generation costs by moving battery investment to earlier years, and therefore, battery operations will reduce generation costs in earlier years by displacing high marginal cost power plants. More specifically, our results indicate California’s bat-

³⁴California’s target under Bill AB 2514 is 1.3 GW of storage power capacity, which equates to 5.2 GWh of storage energy capacity if all battery installations have a 4-hour depth-of-discharge.

tery mandate reduces total expected generation costs by \$511 million in present value terms. Second, a battery mandate increases total capital cost expenditures by moving investments forward in time before expected capital cost declines are realized. Namely, Figure 5 shows that without the battery mandate, expected battery capacity would not reach 5,200 MWh (1,300 MW) until 2043. By moving adoption forward in time, we find that the mandate increases expected capital costs by \$944 million. Notably though, the ex-post total cost of a mandate depends on the speed and extent of future battery capital cost declines. If future battery capital cost reductions turn out to be relatively small, then the ex-post relative total cost of the mandate (i.e., battery capital costs plus generation costs) will be relatively low. However, if future capital cost declines are large, then the ex-post relative cost of the mandate will be bigger. Figure A.7 in Online Appendix A shows the distribution of the total cost from implementing the 5,200 MWh (1,300 MW) mandate relative to the case without a mandate across 10,000 simulated paths from the capital cost distribution. We see that 75% of the time, the mandate increase total cost by less than \$580 million, and 25% of the time the increase is less than \$202 million. About 2% of the time, the mandate reduces total cost because future capital cost reductions end up being much smaller than expected.

Overall, we find the expected change in total costs from meeting California's mandate is relatively small, amounting to \$433 million or about \$11.50 per California resident. Moreover, one of policymakers' main justifications for the mandate in California was that energy storage will help to integrate renewable energy and also improve grid reliability.³⁵ Thus, our estimates suggest that California's mandate policy would be welfare improving if the reliability benefits of energy storage exceed \$433 million by, for instance, helping avoid blackouts during times that electricity demand exceeds available supply. The mean system load during our sample is 24,746 MW. A value of lost load of \$8,000 (Cramton and Lien, 2000) implies a value of \$198 million per hour of system-wide outage averted. Therefore, our estimates suggest that the battery mandate would improve welfare if the batteries were to avert a single system-wide outage for more than 2.2 discounted hours or mitigate a 10% outage for 22 hours discounted over their lifespan.

³⁵Indeed, lawmakers rationalized the mandate—Assembly Bill 2514—on the basis that energy storage will help to integrate renewable energy while maintaining grid reliability.

6 Conclusion

A significant challenge to meeting the world’s growing demand for energy is that utilities cannot typically store electricity for later use. As the majority of new renewable generation capacity comes from intermittent resources, the interest and potential role for battery storage technology has grown substantially. This paper develops a novel dynamic equilibrium model of battery adoption and operations. The model includes a number of key features that we believe are critical for understanding the battery adoption capacity and value created by batteries under different policies. This includes modeling the equilibrium price effects of large-scale battery adoption, ramping costs, depreciation from battery use, and the uncertainty faced by participants in the wholesale electricity market.

We estimate our model using data from California’s electricity market—which allows us to exploit variation in renewable energy generation over time—but our model can be applied to explore the economic impacts of storage in other markets and policy contexts. Our results highlight a number of factors that have first-order impacts on battery storage investment: (1) falling battery capital costs, (2) renewable energy penetration, (3) decreasing marginal value of storage due to equilibrium effects, and (4) battery capacity depreciation.

Although we are currently not very far from a point where a small battery storage investment could break-even in the energy market, expected battery investment could still remain relatively low for decades in the absence of other policy interventions. The largest factor leading to low capacity investment is that batteries flatten electricity price peaks and valleys, thereby limiting the marginal value of additional capacity. While California’s current storage mandate leads to a modest increase in total costs (i.e., battery capital costs plus generation costs) relative to no mandate, it decreases total costs relative to not having a battery market. More ambitious policies to encourage large scale storage will be substantially more costly.

While our analysis makes several contributions towards understanding the economics of battery storage investment, our modeling approach has several limitations. We believe that the most important limitations are as follows. First, our model holds the existing fossil-fuel generation capacity and the associated electricity supply curve constant over time. Second, we use weekly variation in renewable energy over our

4-year sample period and extrapolate to predict the value of storage investment in a world where more renewable generation exist than we can observe within our sample. Third, our base model assumes that future peak load in California remains fixed at 2019 levels. Fourth, our model assumes perfect competition in both traditional generation and storage operations. Fifth, we model battery resources that are operating entirely in the real-time energy market, even though batteries can also offer reserve services. Finally, we assume that battery costs evolve exogenously, and do not allow for battery mandates to lead to declines in production costs through learning-by-doing. As more batteries and renewable resources are deployed in electricity markets, new data will create opportunities to relax some of these assumptions and further investigate still other issues related to the economics of battery storage.

References

- Andrés-Cerezo, D. and Fabra, N. (2020). Storing Power: Market Structure Matters. Cambridge Working Papers in Economics 20122, Faculty of Economics, University of Cambridge.
- Boomhower, J. and Davis, L. (2020). Do energy efficiency investments deliver at the right time? *American Economic Journal: Applied Economics*, 12(1):115–39.
- Brave, S. A., Butters, R. A., and Kelley, D. (2021). A practioner’s guide and MATLAB toolbox for mixed frequency state space modeling. *Journal of Statistical Software*, Forthcoming.
- Bushnell, J. and Novan, K. (2018). Setting with the sun: The impacts of renewable energy on wholesale power markets. Technical report, National Bureau of Economic Research.
- Cole, W. J. and Frazier, A. (2019). Cost projections for utility-scale battery storage. Technical report, National Renewable Energy Lab.(NREL), Golden, CO (United States).
- Cramton, P. and Lien, J. (2000). Value of lost load. Working paper, university of maryland, University of Maryland.
- Cullen, J. A. (2010). Dynamic response to environmental regulation in the electricity industry. In *Industrial Organization Seminar*, page 50.
- Cullen, J. A. and Reynolds, S. S. (2017). Market dynamics and investment in the electricity sector. Technical report, Working paper.
- De Groote, O. and Verboven, F. (2019). Subsidies and time discounting in new technology adoption: Evidence from solar photovoltaic systems. *American Economic Review*, 109(6):2137–72.
- Deaton, A. and Laroque, G. (1992). On the behaviour of commodity prices. *The Review of Economic Studies*, 59(1):1–23.
- Durbin, J. and Koopman, S. J. (2012). *Time Series Analysis by State Space Methods: Second Edition*. Number 9780199641178 in OUP Catalogue. Oxford University Press.
- EIA, U. (2020). Battery storage in the United States: An update on market trends. *Washington, DC: US EIA*.

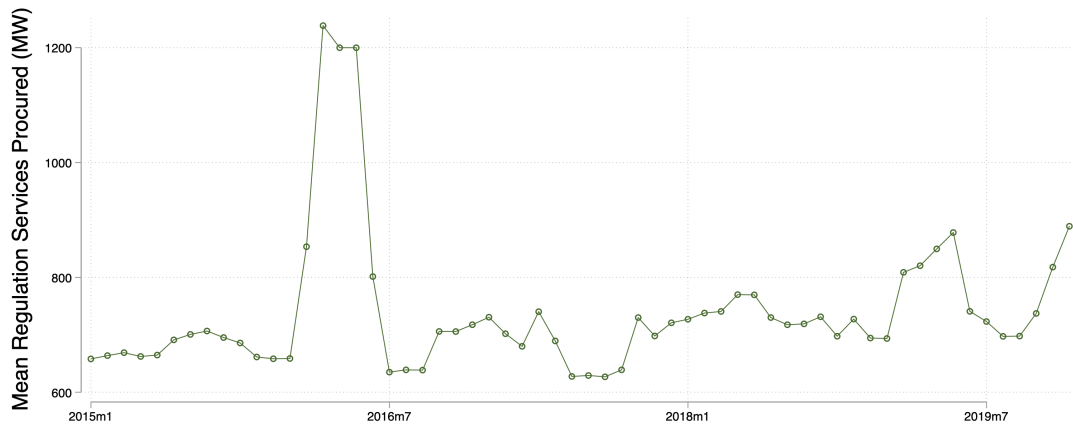
- Feger, F., Pavanini, N., and Radulescu, D. (2017). Welfare and redistribution in residential electricity markets with solar power. Technical Report DP12517, CEPR.
- Goldie-Scot, L. (2019). A behind the scenes take on lithium-ion battery prices. *BloombergNEF*. Available at <https://about.bnef.com/blog/behind-scenes-take-lithium-ion-battery-prices/>.
- Gowrisankaran, G., Reynolds, S. S., and Samano, M. (2016). Intermittency and the value of renewable energy. *Journal of Political Economy*, 124(4):1187–1234.
- Harvey, A. (1989). *Forecasting, Structural Time Series Models and the Kalman Filter*. Cambridge University Press.
- Jha, A. and Leslie, G. (2020). Dynamic costs and market power: Rooftop solar penetration in Western Australia. Available at SSRN 3603627.
- Joskow, P. L. (2011). Comparing the costs of intermittent and dispatchable electricity generating technologies. *The American Economic Review P&P*, 101(3):238–241.
- Kanamura, T. and Ōhashi, K. (2007). A structural model for electricity prices with spikes: Measurement of spike risk and optimal policies for hydropower plant operation. *Energy Economics*, 29(5):1010–1032.
- Karaduman, O. (2021). Economics of grid-scale energy storage in wholesale energy markets. Technical report, M.I.T. Available at: <https://economics.mit.edu/files/18357>.
- Kirkpatrick, A. J. (2018). Estimating congestion benefits of batteries for unobserved networks: A machine learning approach. Technical report, Michigan State University.
- Knittel, C. R. and Roberts, M. R. (2005). An empirical examination of restructured electricity prices. *Energy Economics*, 27(5):791–817.
- Kopecky, K. A. and Suen, R. M. (2010). Finite state Markov-chain approximations to highly persistent processes. *Review of Economic Dynamics*, 13(3):701–714.
- Langer, A. and Lemoine, D. (2018). Designing dynamic subsidies to spur adoption of new technologies. Technical report, National Bureau of Economic Research.
- Ljungqvist, L. and Sargent, T. J. (2012). *Recursive Macroeconomic Theory*. The MIT Press.
- Lucas, R. E. and Prescott, E. C. (1971). Investment under uncertainty. *Econometrica*, 39(5):659–681.
- Mansur, E. T. (2008). Measuring welfare in restructured electricity markets. *The Review of Economics and Statistics*, 90(2):369–386.
- Mokrian, P. and Stephen, M. (2006). A stochastic programming framework for the valuation of electricity storage. Technical report, 26th USAEE/IAEE North American Conference.
- Pirrong, C. (2012). *Commodity Price Dynamics: A Structural Approach*. Cambridge University Press.
- Proietti, T. (2006). Temporal disaggregation by state space methods: Dynamic regression methods revisited. *The Econometrics Journal*, 9(3):357–372.
- Reguant, M. (2014). Complementary Bidding Mechanisms and Startup Costs in Electricity Markets. *The Review of Economic Studies*, 81(4):1708–1742.
- Sackler, D. (2019). New battery storage on shaky ground in ancillary service markets. *Utility Dive*. Available at <https://www.utilitydive.com/news/new-battery-storage-on-shaky-ground-in-ancillary-service-markets/567303/>.

- Sioshansi, R., Denholm, P., Jenkin, T., and Weiss, J. (2009). Estimating the value of electricity storage in PJM: Arbitrage and some welfare effects. *Energy Economics*, 31(2):269–277.
- Tauchen, G. (1986). Finite state markov-chain approximations to univariate and vector autoregressions. *Economics Letters*, 20(2):177–181.
- U.S. Department of Energy (2021). Secretary Granholm announced new goal to cut costs of long duration energy storage by 90 percent. Available at <https://www.energy.gov/articles/secretary-granholm-announces-new-goal-cut-costs-long-duration-energy-storage-90-percent>.
- Weron, R. (2014). Electricity price forecasting: A review of the state-of-the-art with a look into the future. *International Journal of Forecasting*, 30(4):1030–1081.
- Wolak, F. A. (2018). The evidence from California on the economic impact of inefficient distribution network pricing. Technical report, National Bureau of Economic Research.
- Woo, C.-K., Moore, J., Schneiderman, B., Ho, T., Olson, A., Alagappan, L., Chawla, K., Toyama, N., and Zarnikau, J. (2016). Merit-order effects of renewable energy and price divergence in california’s day-ahead and real-time electricity markets. *Energy Policy*, 92:299–312.
- Xu, B., Oudalov, A., Ulbig, A., Andersson, G., and Kirschen, D. S. (2016). Modeling of lithium-ion battery degradation for cell life assessment. *IEEE Transactions on Smart Grid*, 9(2):1131–1140.
- Zhou, Y. and Li, S. (2018). Technology adoption and critical mass: the case of the us electric vehicle market. *The Journal of Industrial Economics*, 66(2):423–480.

Online Appendix

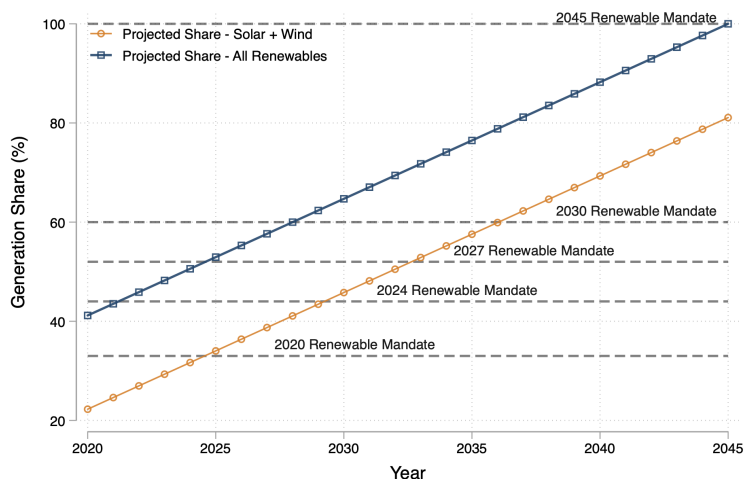
A Additional Tables & Figures Referenced in Main Paper

Figure A.1: Regulation Service Quantity Procured by CAISO



Notes: The figure plots the mean hourly quantity of regulation services procured by CAISO each month. Regulation quantity is calculated the sum of “regulation up” and “regulation down” quantities in the day-ahead market.

Figure A.2: Renewable Energy Over Time Under the California Renewable Portfolio Standard



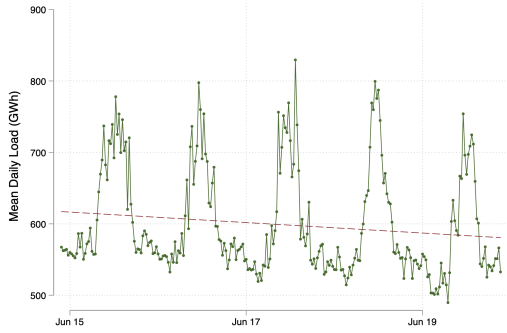
Notes: Each horizontal line shows the share of generation that must come from renewable sources in a particular year under the California RPS. The “All Renewables” line shows our linear interpolation of the California RPS. The “Solar + Wind” line shows our assumption about the solar and wind generation in each year.

Table A.1: Summary Statistics for Estimated Net Load Model

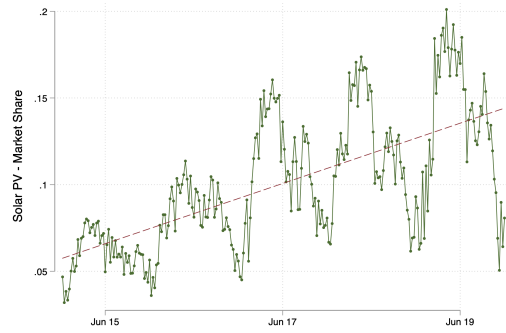
	2015	2016	2017	2018	2019	2016–19
	(a) Dependent Variable: Net Load_t					
Net Load DAM Forecast	0.969 (0.003)	0.950 (0.002)	0.950 (0.001)	0.971 (0.001)	0.955 (0.002)	0.956 (0.001)
Dependent Variable Mean	1794.61	1798.35	1734.13	1687.41	1599.83	1704.99
In-sample RMSE (day-ahead)	67.721	83.007	77.494	74.292	80.513	80.511
	(b) Dependent Variable: ε_t^L					
ε_{t-1}^L	0.996 (0.001)	0.996 (0.000)	0.996 (0.000)	0.995 (0.000)	0.995 (0.000)	0.996 (0.000)
Constant	0.144 (0.043)	-0.014 (0.016)	-0.023 (0.016)	0.178 (0.023)	0.017 (0.021)	0.032 (0.009)
σ_L	6.426	7.110	7.245	7.591	8.131	7.530
Num. Observations	17568	105408	105120	105120	105120	420768

Notes: This table summarizes the estimates of the net load model. The 2015 sample, which is used to obtain the parameters of the AR(1) process, includes only Nov. and Dec. Standard errors, clustered by day-of-sample, are reported in parentheses.

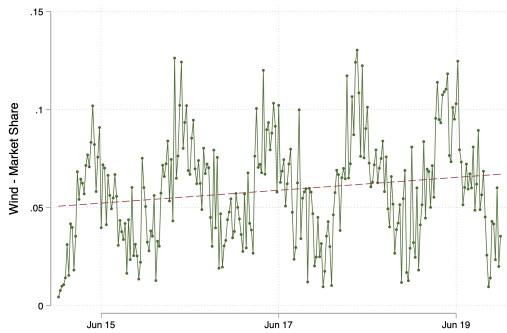
Figure A.3: CAISO Electricity Market Trends



(a) Load



(b) Solar PV Share



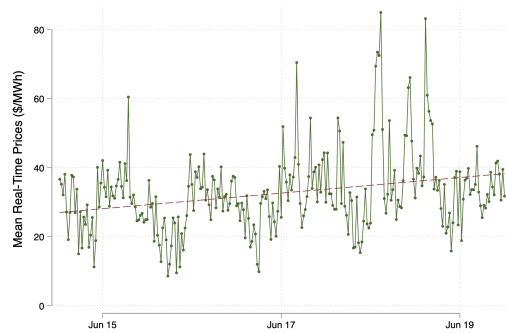
(c) Wind Share



(d) Solar + Wind Share



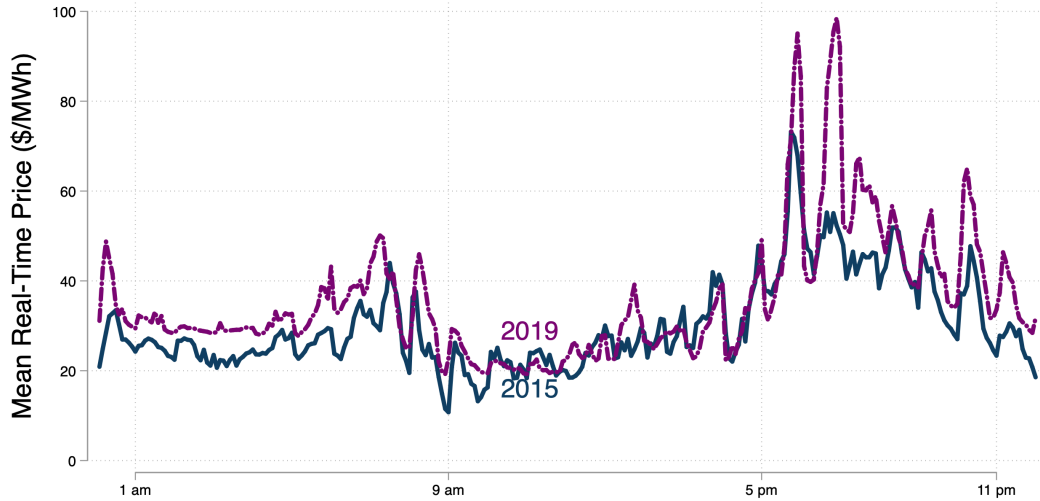
(e) Natural Gas Price (\$/mmbtu)



(f) RTM Price (\$/MWh)

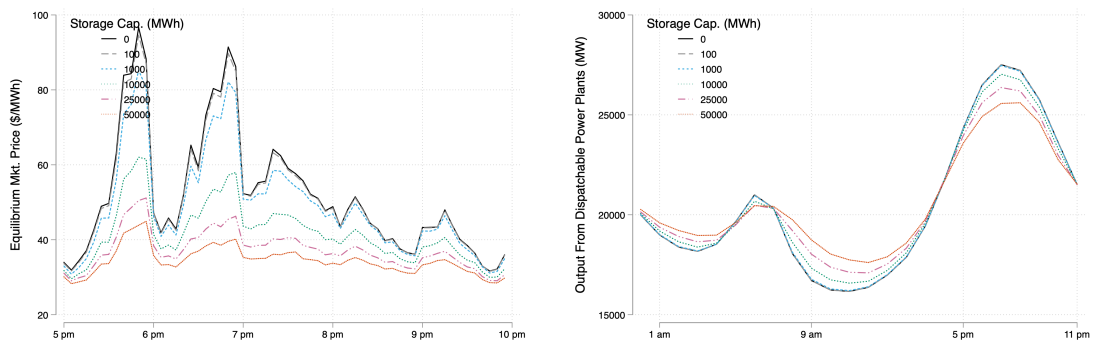
Notes: Each graphic plots the weekly average of a given single variable over the sample period. The solar generation measure does not include distributed generation. The reported market prices are for the CAISO South Zone Trading Hub (SP 15). All data collected from CAISO.

Figure A.4: Real-Time Market Prices (5-Minute Frequency)



Notes: Figure shows the average real-time market price (South Hub - SP-15) for each 5-minute interval of the day, separately for 2015 and 2019.

Figure A.5: Equilibrium Prices Effects and Dispatchable Generator Output



(a) Peak Five-Minute Equilibrium Prices

(b) Mean Hourly Output from Dispatchable Generators

Notes: Each line plots the mean counterfactual outcome for specific storage capacity level across all days during 2016–19.

Table A.2: Summary Statistics for Estimated Marginal Cost Curve Parameters

Parameter	2015	2016	2017	2018	2019	2016–19
θ_1						
Mean	-14.59	-15.85	-10.96	-7.92	-8.64	-10.85
Std. Dev.	20.79	19.58	15.67	12.22	12.78	15.64
25th-percentile	-15.75	-30.38	-11.50	-6.57	-7.42	-9.95
75th-percentile	-2.05	-2.29	-1.73	-1.69	-2.01	-1.95
θ_2						
Mean	76.30	88.82	57.07	36.13	40.96	55.77
Std. Dev.	148.17	144.35	111.87	87.27	92.63	113.11
25th-percentile	0.82	0.94	0.62	0.77	0.71	0.76
75th-percentile	35.46	134.63	26.10	10.10	10.98	21.79
θ_3						
Mean	1.60	1.41	1.42	1.53	1.28	1.41
Std. Dev.	1.20	0.99	0.97	1.09	0.81	0.97
25th-percentile	1.01	1.01	1.01	1.01	1.01	1.01
75th-percentile	1.01	1.01	1.01	1.01	1.01	1.01
κ						
Mean	2.99	3.32	2.87	2.53	2.61	2.83
Std. Dev.	2.43	2.73	2.46	2.09	2.29	2.42
25th-percentile	1.43	1.33	1.28	1.32	1.28	1.29
75th-percentile	3.18	5.32	3.08	2.38	2.39	2.91
α						
Mean	0.84	0.87	0.83	0.84	0.82	0.84
Std. Dev.	0.10	0.10	0.13	0.13	0.13	0.12
25th-percentile	0.77	0.80	0.74	0.77	0.73	0.77
75th-percentile	0.91	0.97	0.95	0.94	0.93	0.95

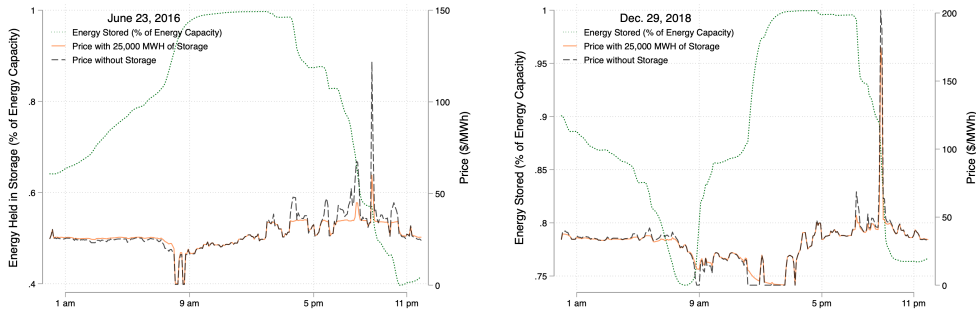
Notes: This table summarizes the means, standard deviations, 25th and 75th percentile of the daily estimated marginal cost curve parameters.

Table A.3: Summary Statistics for Estimated Marginal Cost Curve Residuals

	2015	2016	2017	2018	2019	2016–19
	Dependent Variable: ε_t^P					
ε_{t-1}^P	0.869 (0.030)	0.896 (0.013)	0.880 (0.015)	0.907 (0.012)	0.838 (0.016)	0.891 (0.008)
Constant	0.019 (0.004)	0.011 (0.001)	0.013 (0.002)	0.011 (0.001)	0.009 (0.001)	0.011 (0.001)
$\sigma^{P,Peak}$	0.015	0.012	0.013	0.015	0.017	0.014
$\sigma^{P,Off-peak}$	0.013	0.010	0.012	0.012	0.015	0.012
Num. Observations	17568	105408	105120	105120	105120	420768

Notes: This table summarizes the estimates of the marginal cost curve residual parameters. The 2015 sample includes only Nov. and Dec. Standard errors, clustered by day-of-sample, are reported in parentheses.

Figure A.6: Battery Operations on Selected Days



Notes: The black lines show the observed real-time market price in the absence of battery operations. The orange lines show the equilibrium prices after incorporating storage operations. The green lines in both show the simulated amount of energy held in storage (i.e. the stock) as a percentage of energy capacity on June, 23, 2016 and December, 29, 2018. The simulations use an aggregate storage capacity of 25,000 MWh.

Table A.4: Equilibrium Prices and Aggregate Battery Capacity

	Price (All hours)	Price (6-9 AM)	Price (10 AM - 3 PM)	Price (5-10 PM)
0	35.97	31.52	25.23	54.27
10	35.95	31.51	25.23	54.21
100	35.77	31.40	25.17	53.72
1000	34.79	30.83	24.87	51.15
5000	33.14	30.00	24.73	46.46
10000	31.99	29.31	24.91	42.94
15000	31.42	29.08	25.24	40.90
25000	30.63	28.56	25.74	38.22
50000	29.62	28.24	25.51	35.25

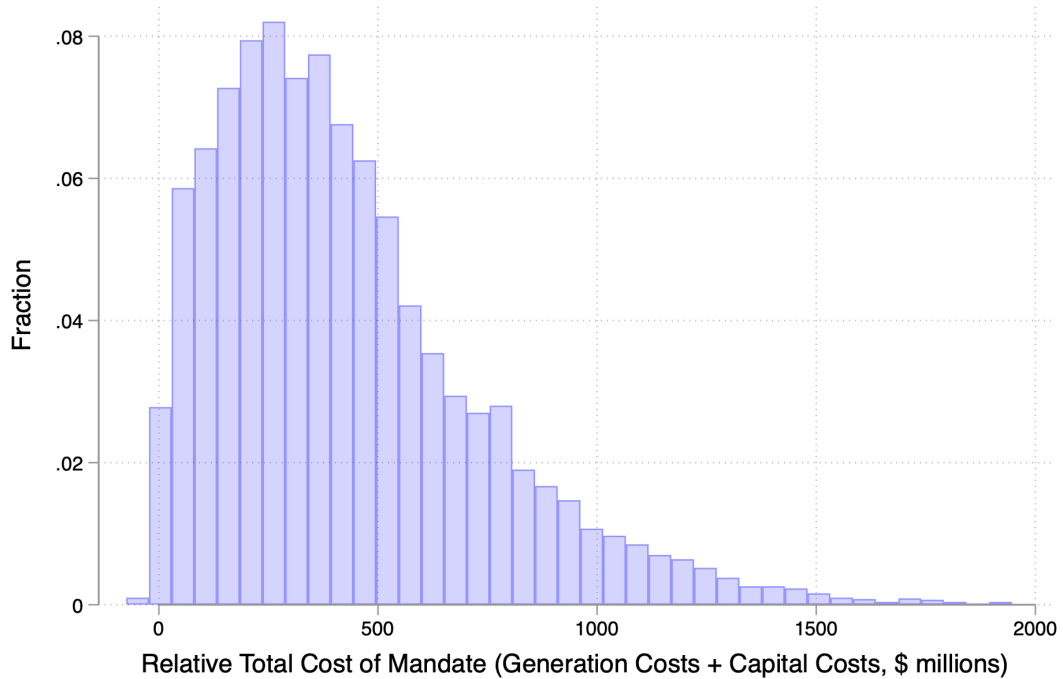
Notes: Prices reported are in \$/MWh and are the load-weighted mean across all five minute intervals between 2016–19.

Table A.5: Skewed Distribution of Battery Revenues Across Time Periods

	Time Periods - Other Percentiles	Time Periods - 99th Percentile
Battery Capacity in MWh: 10	15,996.72	41,948.91
Battery Capacity in MWh: 100	15,993.46	41,171.26
Battery Capacity in MWh: 1000	16,762.16	37,395.82
Battery Capacity in MWh: 5000	14,518.92	30,495.52
Battery Capacity in MWh: 10000	12,852.22	26,891.49
Battery Capacity in MWh: 15000	10,752.46	24,265.86
Battery Capacity in MWh: 25000	8,681.60	20,800.56
Battery Capacity in MWh: 50000	5,374.76	15,469.13

Notes: The first column lists the aggregate battery capacity. The second column indicates the total revenue a battery owner would earn between 2016–19 summed over the least profitable 99 percent of time periods. The third column lists the total revenue a battery owner would earn summed over the most profitable 1 percent of time periods. All numbers are in \$/MWh of capacity.

Figure A.7: Total Cost Distribution with 5,200 MWh Mandate Relative to No Mandate



Notes: We calculate the difference in ex-post discounted total costs (generation costs plus battery capital costs), with and without a 5,200 MWh (1,300 MW) mandate across 10,000 different simulated paths of the capital cost distribution.

Table A.6: Robustness Checks: Social Value of Storage as a Function of Storage Capacity and Renewables

	Gross Social Surplus / K (\$/kWh)			
	(1)	(2)	(3)	(4)
ln(K)	-8.220*** (2.748)	-8.220*** (2.748)	-8.220*** (2.749)	-8.220*** (2.748)
Renewable Share (%)	8.183* (4.395)	8.779* (4.680)	8.342* (4.809)	16.99 (13.99)
ln(K) × Renewable Share (%)	-0.6855*** (0.1653)	-0.6855*** (0.1653)	-0.6855*** (0.1653)	-0.6855*** (0.1653)
Peak Load (Mean)	0.1568* (0.0930)		0.1353 (0.2180)	
Load (Mean)		0.2172 (0.1317)		
Off-Peak Load (Mean)			0.0358 (0.3410)	
(Renewable Share) ²				-0.3166 (0.3212)
Observations	1,664	1,664	1,664	1,664
R ²	0.39122	0.39093	0.39124	0.38622
Within R ²	0.16075	0.16035	0.16078	0.15385
Controls + week of year fixed effects	✓	✓	✓	✓

Notes: The dependent variable is the present discounted social surplus per kWh of storage capacity, not accounting for capacity depreciation. Each observation represents a single week of the sample for a single storage capacity. All columns include controls for the mean natural gas price over the week and the Sacramento Valley hydroelectric water year index (WYI) associated with that week. Peak load is the mean load between 5pm and 9pm hours during the week; off-peak load is the mean load at all other times. Standard errors are clustered by week of sample.

B The Kalman Filter/Smoothen

As described in Section 4.1, a complication of our data is that CAISO implements the day-ahead market (DAM) only at the hourly frequency, reporting prices and forecasts for net load that are constant over the 12 5-minute intervals of each hour. Our operations model and the real-time market (RTM) prices use a 5-minute frequency. Thus, our estimation procedure needs to accommodate the mixed-frequency nature of the data.

We use the Kalman filter/smoothen to temporally disaggregate (i.e., interpolate) the forecasts of net load to yield a forecast at the 5-minute frequency. Generically, assume that a series A_t is observed only every h periods, and what is observed is the average of the interim h periods of the latent process a_t , so $A_t = \frac{1}{h} \sum_{j=0}^{h-1} a_{t-j}$. Our objective is to take the observed series A_t and construct estimates of the latent process a_t such that the implied values of the accumulated version of that series, ϕ_t , match the observable data (A_t) at the end of the h periods. We cast the problem as a state space model and use the Kalman filter/smoothen to estimate the latent process (e.g., [Proietti, 2006](#)).

More specifically, we use the following state space model:

$$A_t = H_t \begin{bmatrix} a_t \\ \phi_t \end{bmatrix},$$

$$\begin{bmatrix} a_t \\ \phi_t \end{bmatrix} = M_t \begin{bmatrix} a_{t-1} \\ \phi_{t-1} \end{bmatrix} + U_t \psi_t, \quad \psi_t \sim N(0, 1),$$

where H_t is a deterministically time-varying selection matrix³⁶ designed to handle the missing observations of A_t ; M_t ³⁷ and U_t ³⁸ are deterministically time-varying matrices designed to create the accumulated version of the latent process, ϕ_t ; and ψ_t is a serially independent error term that contributes to the time series variation in the latent pro-

³⁶ H_t iterates between the matrix $[0 \ 1]$ on the last period of each hour (the period we observe A_t , and $[0 \ 0]$ for the first to penultimate period of each hour.

³⁷ M_t takes 12 possible values for each period within the hour such that $M_t = [1 \ 0; 1/j(t) \ (j(t) - 1)/j(t)]$, where $j(t)$ is the period within the hour associated with time period t .

³⁸ U_t takes 12 possible values for each period within the hour such that $U_t = [1; 1/j(t)]$, where $j(t)$ is the period within the hour associated with time period t .

cess of interest a_t . We use the techniques outlined in [Harvey \(1989\)](#) and [Durbin and Koopman \(2012\)](#) to recover an estimate of the latent a_t for each five minute interval in our sample.³⁹ We then use these estimates to augment our data on the deterministic portion of net load, X_s^L .

AB/JD: changed title.

C Details of Estimation of Electricity Generation Costs

We use the net load and price data from the day-ahead market (DAM) to estimate daily supply curve parameters. Variation in these parameters over time may be caused by shifts in natural gas prices, changes in the availability of low cost generation coming from nuclear power plants and hydroelectric sources, as well as day-to-day changes in generator availability and imports and exports from neighboring states. By using the DAM to estimate the marginal cost curve, our approach allows us to account for market characteristics that vary at a high frequency, while ensuring that our dynamic operations model remains feasible in that it only uses information that would be available to a market participant in bidding in the real-time market.

Given the definition of total costs in (6) and the functional form for marginal costs in (11), total costs are equal to:

$$\begin{aligned}
 TC(q, s, \tilde{Z}, \varepsilon^L, \varepsilon^P) &= \theta_1 Z - \frac{\theta_2 \left[\exp(\varepsilon^P) \kappa^\alpha \tilde{Z}^{1-\alpha} - Z \right]^{1-\theta_3}}{1 - \theta_3}, \\
 &+ \frac{\theta_2 \left[\exp(\varepsilon^P) \kappa^\alpha \tilde{Z}^{1-\alpha} \right]^{1-\theta_3}}{1 - \theta_3}, \text{ where } Z = X_s^L - Q(q) + \varepsilon^L.
 \end{aligned} \tag{C.1}$$

³⁹See [Brave et al. \(2021\)](#) for the explicit recursive formulation of the Kalman filter/smoothing equations for a temporally aggregated series involving an average.

We model the transition of ε^P as an AR(1) process given by:

$$\begin{aligned}\varepsilon_t^P &= \rho^P \varepsilon_{t-1}^P + \sigma_{s(t)}^P \eta_t^P \\ \sigma_{s(t)}^P &= \begin{cases} \sigma^{P,\text{Peak}} & \text{if } s(t) \in \text{Hours 5-10pm} \\ \sigma^{P,\text{Off-peak}} & \text{if } s(t) \notin \text{Hours 5-10pm} \end{cases},\end{aligned}\tag{C.2}$$

where η^P is a mean zero serially uncorrelated shock with unit variance, ρ^P governs the persistence of changes to available capacity, and $\sigma_{s(t)}$ accommodates any heteroskedasticity that exists across peak (5pm-10pm) and off-peak hours of the day.

To facilitate estimation, we also standardize each day's DAM prices and net load forecasts. For the DAM prices, we subtract the median and divide by its interquartile range. For net load, we divide by the maximum of that day's net load forecast. Finally, we restrict the parameter domain, Θ , to be such that $\theta_1 \in [-700, 500]$, $\theta_2 \in [0, 500]$, $\theta_3 \in [1.01, 4]$, $\kappa \in [1, 8]$, $\alpha \in [0, 1]$.⁴⁰

Turning to the structural unobservable, conditional on a set of supply curve parameters for any particular day, we recover a time series of ε_t^P as the shocks required to rationalize the RTM price observed at time t with the realizations of net load and lagged net load. At time t , we obtain:

$$\varepsilon_t^P = \ln \left[Z_t + \left(\frac{P_t^{RTM} - \theta_1}{\theta_2} \right)^{-1/\theta_3} \right] - \ln \left[\kappa^\alpha \tilde{Z}_t^{1-\alpha} \right],\tag{C.3}$$

where we use the day d estimated values of (θ, κ, α) .

To account for the possibility of heteroskedasticity, we estimate separate variances for peak and off-peak periods.⁴¹ We also estimated the ρ^P , $\sigma^P(\text{Peak})$, $\sigma^P(\text{Off-Peak})$ parameters separately for each year in our sample and found that these parameters are relatively constant over time, see Table A.3 in Online Appendix A.

Table A.2 in Online Appendix A reports sample statistics on the marginal cost curve parameters. The linear marginal cost parameter, θ_1 , is below zero for the large majority of days. The weights on the current capital in the Cobb-Douglas capital func-

⁴⁰We also compute a perfect foresight model, which uses the same marginal cost curve parameters.

⁴¹For our estimates of $\sigma^P(\text{Peak})$, $\sigma^P(\text{Off-Peak})$, we use a robust (and consistent) estimator of the scale for the normal distribution: $1.4826 \times \text{median}_t\{|x_t - \text{median}_j x_j|\}$ (?).

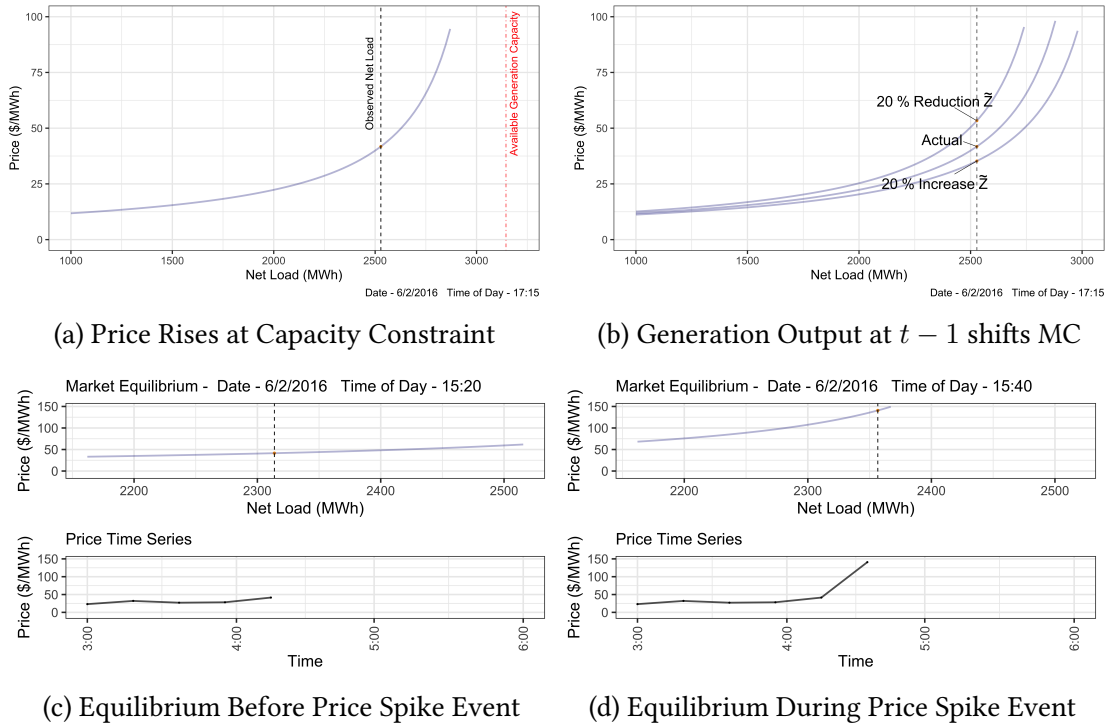
tion, α , center around 0.80 and are fairly stable, indicating the presence of positive and similar ramping costs throughout our sample. Consistent with the declining natural gas prices, the average slope of the marginal cost curve, θ_2 , falls over our sample period, although there is significant within-year volatility. Finally, estimates for θ_3 and κ indicate that the curvature of the marginal cost curve and the scheduled available capacity are relatively stable over our analysis sample.

Table A.3 reports our parameter estimates for the AR(1) process for ε^P . Our estimate of ρ^P —based off the training sample of 2015—is 0.869. Thus, shocks to available generating capacity exhibit less persistence than the shocks to net load. This level of persistence is also stable over the evaluation sample—lying within a range of 0.838 to 0.907. Our estimates of the standard deviations for on- and off-peak from our training sample are 0.015 and 0.13, respectively. These estimates exhibit stability over our evaluation sample—never deviating more than 24 percent from our training sample estimates. Across both the training and evaluation samples, the estimates of $\sigma^P(\text{Peak})$, $\sigma^P(\text{Off-Peak})$ indicate that on-peak hours experience approximately 15 percent more volatile changes in ε^P .

As an example of the features of our approach towards modeling marginal costs, Figure C.1 provides the marginal cost curve on June 2, 2016, when net load was approaching the constraint on available generating capacity. From Figure C.1a, at 5:15 pm, the market equilibrium was near an inflection point: an increase in net load would significantly raise equilibrium price, while a decrease in net load would only have a small effect in decreasing price. Figure C.1b illustrates the importance of ramping costs in our model. At this same time, a 20% decrease in generation from fossil fuel generators last period (\tilde{Z}) would lead to a substantial price increase, with a smaller price decrease from a 20% increase in \tilde{Z} .

Figures C.1c and C.1d illustrate how our model rationalizes a rapid change in price that occurred in the real-time market. At 3:20 pm on June 2, 2016, the real-time market price was just under \$50/MWh, then at 3:40 pm price nearly tripled to \$140/MWh. As evidenced by the change in the marginal cost curves between 3:20 pm (top sub-panel of c) and 3:40 pm (top sub-panel of d), the model largely rationalizes this price change as being due to a shock in the available generating capacity, ε_t^P , (as opposed to an anticipated or unanticipated movement along the curve driven by net load), perhaps

Figure C.1: Time-Varying Marginal Cost Curve

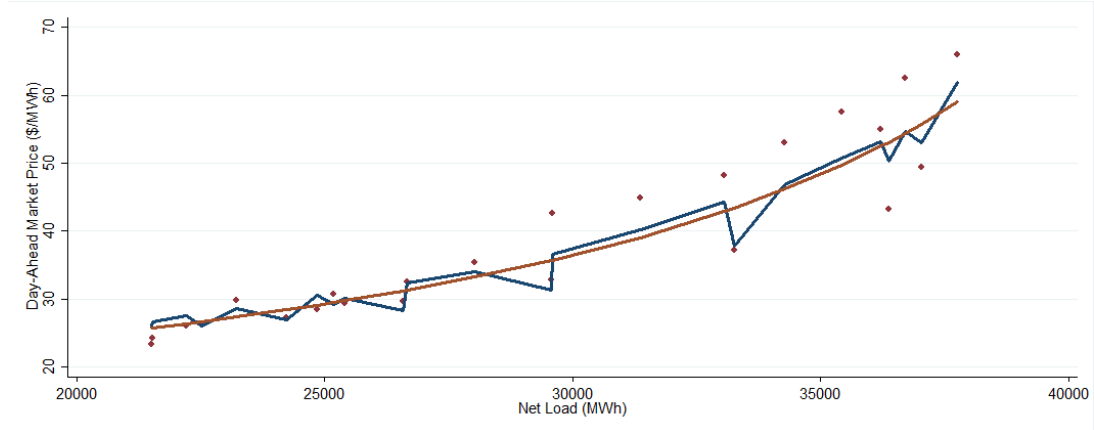


Notes: This figure displays marginal cost curves for June 2, 2016. Figure C.1a shows the market equilibrium and the implied generation capacity available for a single five-minute interval. Figure C.1b shows how 20% changes in last period's dispatchable generation would shift the marginal cost curve. Figures C.1c and C.1d show how both the net load and the marginal cost curve shifts during a period when price increased rapidly over a 20-minute span.

due to unplanned generator outages or a transmission congestion event.

Figure C.2 provides the fit of the supply curve for June 28, 2016. The maroon dots show the net load forecasts and DAM price realizations. The blue line shows the predicted DAM prices as a function of the forecasts of net load from our estimated model. Finally, the orange line shows the predicted DAM prices as a function of the forecasts of net load from a model estimated without ramping costs (i.e., $\alpha = 1$). By allowing for ramping costs, the blue line is able to explain more of the variation in the DAM prices than the orange line, and hence lies closer to the maroon dots.

Figure C.2: Marginal Cost Curve From Day-Ahead Market



Notes: This figure displays the day-ahead market prices and forecast of net load for each hour for June 28, 2016. Additionally, the figure displays the estimated marginal cost curve with ramping costs (blue line) and without ramping costs (orange line). The reported market prices are for the CAISO South Zone Trading Hub (SP 15).

D Modeling Battery Capacity Depreciation

We model capacity fading or depreciation using [Xu et al. \(2016\)](#). In their approach, the depreciation rate of a battery is a non-linear function of time and cycling. Specifically, depreciation depends on: (1) temperature, (2) depth-of-discharge, (3) state-of-charge, (4) calendar time, and (5) number of cycles. For our application, we assume that batteries are operated at 25°C (77°F) throughout the year, which is the [Xu et al.](#) base case.

Let K denote the battery's capacity this period, K' denote its capacity next period,⁴² and g_d be the term that determines degradation between the current period and next period, so that:

$$K' = K \exp(-g_d). \quad (\text{D.1})$$

From [Xu et al. \(2016\)](#), g_d consists of calendar degradation and cycle degradation.

The first component of the degradation function, calendar degradation g_t , is the portion that occurs regardless of how much the battery is charged or discharged. Calendar degradation is a function of elapsed time as well as the battery's mean state-of-charge. Battery capacity will degrade more if the battery is left idle at full state-of-charge relative to if the battery is left idle at 50% state-of-charge. More concretely, at

⁴²Our evaluation sample uses a period length of a week, as we discussed in Section 4.2.

25°C, calendar degradation is the following function of elapsed time in seconds, \tilde{t} , and the mean state-of-charge during the time elapsed, $\bar{\sigma}$:

$$g_t = 0.000000000414 \times \tilde{t} \times \exp(1.04(\bar{\sigma} - 0.5)). \quad (\text{D.2})$$

The second component of the degradation function, cycle degradation, is the depreciation attributable to operations. Using the [Xu et al.](#) notation, define N to be the total number of cycles that the battery undertakes during a time period, where a full cycle indicates a battery making a roundtrip of charging and discharging; n_i to indicate if cycle i was a full roundtrip cycle ($n_i = 1$) or a half cycle ($n_i = 0.5$) of either charge or discharge; and g_{ci} to be the cycle degradation during cycle i . The cycle degradation g_{ci} depends on the mean state-of-charge during cycle i , σ_i , as well as the depth of discharge of the cycle, δ_i . The depth of discharge indicates what fraction of power was gained or lost during the cycle. Cycle degradation is convexly increasing in the depth of discharge. E.g., cycling from 0% to 100% once is more damaging than cycling from 25–75% twice. Applying [Xu et al. \(2016\)](#) to the case of 25°C,

$$g_{ci} = \exp(1.04(\sigma_i - 0.5)) \times (140000\delta_i^{-0.501} - 123000)^{-1}. \quad (\text{D.3})$$

We combine the different degradation terms to write:

$$g_d = g_t + \sum_i^N n_i g_{ci}. \quad (\text{D.4})$$

From (D.2)–(D.4), capacity depreciation g_d is a function of \tilde{t} , N , $\bar{\sigma}$, and n_i, δ_i , and $\sigma_i, \forall i = 1, \dots, N$.

Following [Xu et al. \(2016\)](#), we perform the following algorithm to simulate capacity depreciation for our evaluation sample:⁴³

1. Solve the optimal policy for a given week. Recall that we solve for policies separately for each day within the week and that our policy functions for the evaluation sample incorporate a heuristic approach that limits cycling due to depreciation.

⁴³Our algorithm for the training sample is similar, but occurs over the entire 2015 training sample period—rather than separately by each week—and uses perfect foresight policies.

2. Use the optimal policy from (1) and the realized stream of load residuals ε^L , price residuals ε^P , and supply curve parameters across all time periods in the week to simulate charge/discharge actions.
 - Record the batteries' state-of-charge for each 5-minute time interval of the simulation.
3. Calculate g_t over the simulation period using (D.2).
 - Use the recorded state-of-charge path to calculate the mean state-of-charge over the simulation period, $\bar{\sigma}$.
 - Over one week, $\tilde{t} = 60 \times 60 \times 24 \times 7 = 604,800$.
4. Feed the recorded state-of-charge path into a rainflow cycle counting algorithm.
 - See <https://www.mathworks.com/matlabcentral/fileexchange/3026-rainflow-counting-algorithm>.
 - The rainflow counting algorithm returns N and n_i, δ_i , and $\sigma_i, \forall i = 1, \dots, N$. In words, it returns the number of cycles and whether each cycle is full or half, and determines the depth-of-discharge and mean state-of-charge for each cycle.
5. Calculate $g_{ci}, \forall i = 1, \dots, N$ using (D.3).
6. Calculate the total depreciation rate $\exp(-g_d)$ for each week-long simulation using the above estimates and (D.4) and (D.1).

Finally, we note that this formulation implicitly assumes that both power and energy capacity depreciate through cycling. The engineering literature shows that primarily energy capacity should degrade. Therefore, our calculation should provide a lower bound on the social value of storage.

E Details of Estimation of Battery Capital Costs

We treat the first year of our sample, 2018, as $y = 0$. We rescale costs in year y to be relative to initial cost c_0 , so that $\tilde{c}_y \equiv c_y/c_0$. Taking logs of both sides of the (rescaled)

capital cost evolution equation (15) from Section 4.3, we obtain:

$$\ln(\tilde{c}_y) - \underbrace{\ln(\tilde{c}_0)}_{\ln 1=0} = \tau \times y + \sum_1^y \xi_y. \quad (\text{E.1})$$

Using (E.1), we derive the following moment conditions.

First moment:

$$E[\ln(\tilde{c}_y)] = \tau \times y. \quad (\text{E.2})$$

Second moment:

$$\begin{aligned} \text{Var}[\ln(\tilde{c}_y)] &= \text{Var}\left[y\tau + \sum_1^y \xi_y\right] \\ \Rightarrow \text{Var}[\ln(\tilde{c}_y)] &= \text{Var}[y\tau] + \text{Var}\left[\sum_1^y \xi_y\right] \\ &\Rightarrow \text{Var}[\ln(\tilde{c}_y)|y] = y \times \text{Var}[\xi_y] \\ &\Rightarrow \text{SD}[\ln(\tilde{c}_y)|y] = \sqrt{y} \times \text{SD}[\xi_y] \\ &\Rightarrow \text{SD}[\ln(\tilde{c}_y)|y] = \sqrt{y} \times \sigma. \end{aligned} \quad (\text{E.3})$$

We find the parameters τ and σ_c that solve the two moment conditions by estimating two univariate regressions, pooling across the set of cost projections. For the first regression the dependent variable is $\ln(\tilde{c}_y)$, and the independent variable is y . For the second regression, the dependent variable is the standard deviation of all the logged cost realizations $\ln(\tilde{c}_y)$ conditional on y and the independent variable is \sqrt{y} . To accommodate the variation in the number of cost assessments over time, in the second regression we weight the regression by the number of cost projections that were made for that year.⁴⁴

⁴⁴Figure 2a shows that years that are further in the future tend to have fewer cost projections.